Title

Exploratory Technology Research Program for Electrochemical Energy Storage - Annual Report for 1998

Author

Kinoshita (Editor), K.

Publication Date

1999-06-01

Exploratory Technology Research Program for Electrochemical Energy Storage

Annual Report for 1998

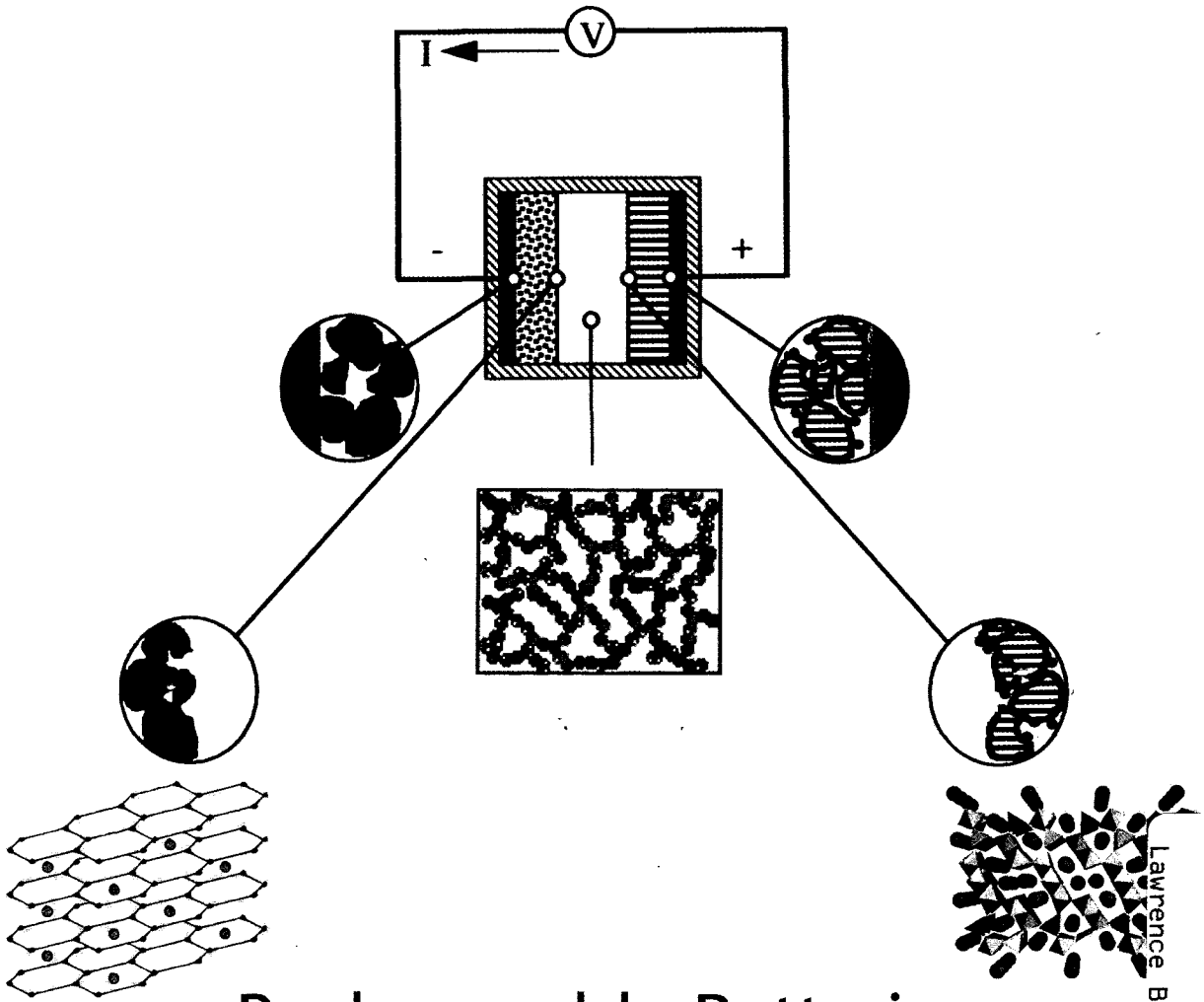

Rechargeable Batteries for Electric and Hybrid Vehicles

Energy Efficiency and Renewable Energy • Office of Transportation Technologies • Office of Advanced Automotive Tech

ABOUT THE COVER:
Schematic illustration of a rechargeable lithium battery showing (from left to right) the current collector/negative electrode interface, the negative electrode, a composite electrolyte, the positive electrode, and the positive electrode/current collector interface. A current, I, flows through the external circuit, and the cell delivers a voltage, V.

DISCLAIMER

LBNL-42694

EXPLORATORY TECHNOLOGY RESEARCH PROGRAM FOR ELECTROCHEMICAL ENERGY STORAGE

ANNUAL REPORT FOR 1998

Environmental Energy Technologies Division
Lawrence Berkeley National Laboratory
University of California
Berkeley, California 94720

Edited by Kim Kinoshita, Technical Manager

June 1999

This work was supported by the Assistant Secretary for Energy Efficiency and Renewable Energy, Office of Transportation Technologies, Office of Advanced Automotive Technologies of the U.S. Department of Energy under Contract No. DE-AC03-76SF00098.

CONTENTS

INTRODUCTION 1

RESEARCH PROJECT SUMMARIES 2

ELECTRODE CHARACTERIZATION

Carbon Electrochemistry 2
K. Kinoshita (Lawrence Berkeley National Laboratory)

Fabrication and Testing of Carbon Electrodes as Lithium-Intercalation Anodes 5
T.D. Tran (Lawrence Livermore National Laboratory)

Safety and Reactivity of Carbonaceous Anodes Used in for Lithium-Ion Technology 6
M.D. Curtis and G.A. Nazri (University of Michigan and GM Research and Development Center)

Battery Materials: Structure and Characterization 9
J. McBreen (Brookhaven National Laboratory)

ELECTRODES FOR AQUEOUS ELECTROCHEMICAL CELLS

Preparation of Improved, Low-Cost Metal Hydride Electrodes for Automotive Applications 11
J.J. Reilly (Brookhaven National Laboratory)

Optimization of Metal Hydride Properties in MH/NiOOH Cells for Electric Vehicles 14
R.E. White (University of South Carolina)

Microstructural Modeling of Highly Porous MH/NiOOH Battery Substrates 16
A.M. Sastry (University of Michigan)

COMPONENTS FOR NONAQUEOUS CELLS

Novel Lithium/Polymer-Electrolyte Cells 19
E.J. Cairns and F.R. McLarnon (Lawrence Berkeley National Laboratory)

New Cathode Materials 21
M.S. Whittingham (State University of New York at Binghamton)

Solid Electrolytes 23
L.C. De Jonghe (Lawrence Berkeley National Laboratory)

Polymer Electrolyte Synthesis for High-Power Batteries 27
J.B. Kerr (Lawrence Berkeley National Laboratory)

Composite Polymer Electrolytes for Use in Lithium and Lithium-Ion Batteries 29
S. Khan and P.S. Fedkiw (North Carolina State University)

Polymer Electrolytes for Ambient-Temperature Traction Batteries: Molecular-Level Modeling for Conductivity Optimization 31
M.A. Ratner (Northwestern University)

Corrosion of Current Collectors in Rechargeable Lithium Batteries 33
J.W. Evans (Lawrence Berkeley National Laboratory/University of California at Berkeley)

Development of Novel Chloroaluminate Electrolytes for High-Energy-Density Rechargeable Lithium Batteries 34
K.A. Wheeler (Delaware State University)

CROSS-CUTTING RESEARCH

Analysis and Simulation of Electrochemical Systems 36
J.S. Newman (Lawrence Berkeley National Laboratory/University of California at Berkeley)

Electrode Surface Layers 39
F.R. McLarnon (Lawrence Berkeley National Laboratory)

Lithium Electrode Interfacial Studies 42
P.N. Ross, Jr. (Lawrence Berkeley National Laboratory)

ACKNOWLEDGMENTS 44

ACRONYMS 44

LIST OF PRIOR ANNUAL REPORTS 46

FINANCIAL DATA 47

INTRODUCTION

The U.S. Department of Energy's (DOE) Office of Advanced Automotive Technologies conducts research and development on advanced rechargeable batteries for application in electric vehicles (EVs) and hybrid systems. Efforts are focused on advanced batteries that offer the potential for high performance and low life-cycle costs, both of which are necessary to permit significant penetration into commercial markets.

DOE battery R&D supports two major programs: the United States Advanced Battery Consortium (USABC), which develops advanced batteries for EVs, and the Partnership for a New Generation of Vehicles (PNGV), which seeks to develop passenger vehicles with a fuel economy equivalent to 80 mpg of gasoline. This report describes the activities of the Exploratory Technology Research (ETR) Program, managed by the Lawrence Berkeley National Laboratory* (LBNL). The role of the ETR Program is to perform supporting research on the advanced battery systems under development by the USABC and PNGV Programs, and to evaluate new systems with potentially superior performance, durability and/or cost characteristics. The specific goal of the ETR Program is to identify the most promising electrochemical technologies and transfer them to the USABC, the battery industry and/or other Government agencies for further development and scale-up. This report summarizes the research, financial and management activities relevant to the ETR Program in CY 1998. This is a continuing program, and reports for prior years have been published; they are listed at the end of this Program Summary.

---

* Participants in the ETR Program include the following LBNL scientists: E. Cairns, J. Evans, J. Kerr, K. Kinoshita, F. McLarnon and J. Newman of the Environmental Energy Technologies Division; and L. De Jonghe and P. Ross of the Materials Sciences Division.

RESEARCH PROJECT SUMMARIES

ELECTRODE CHARACTERIZATION

Characterization of electrode morphology and chemical composition are important for the successful development of rechargeable electrodes for advanced secondary batteries. Efforts are underway to utilize advanced fabrication techniques and spectroscopy to characterize electrode properties.

Carbon Electrochemistry

Kim Kinoshita
90-1142, Lawrence Berkeley National Laboratory, Berkeley CA 94720
(510) 486-7389; fax: (510) 486-4260; e-mail: k_kinoshita@lbl.gov

Objective

- Identify the critical parameters that control the reversible intercalation of Li in carbonaceous materials and determine their maximum capacity for Li intercalation.

Approach

- Couple electrochemical studies with physical measurements to correlate the relationship between the physicochemical properties of carbonaceous materials and their ability to intercalate Li.
- Apply thermal analysis and microscopy techniques to characterize the structure of carbon materials for Li-ion batteries.

Accomplishments

- Thermal analysis (TGA and DTA) involving air oxidation of carbons and electrochemical studies suggest that the active surface area, and not the total BET surface area, has an influence on the irreversible capacity loss of carbons for Li-ion batteries.

Future Directions

- Continue collaboration with Superior Graphite and University of Michigan to identify a low-cost carbon with improved rate capability in Li-ion batteries.
- Continue *in situ* ellipsometry studies of lithiated carbons, and determine the relationship between the type of carbon and the properties of the surface layer formed during the first charge cycle.

The objective of this project is to identify the critical parameters that control the reversible intercalation of Li in carbonaceous materials. This project involves investigations of the role of physicochemical properties of carbonaceous materials on their ability to reversibly intercalate Li. This latter effort is coordinated with the research conducted at University of Michigan to evaluate the reactions that occur during electrolyte decomposition at carbon electrodes in Li-ion batteries (see discussion in "Reactivity and Safety Aspects of Carbonaceous Anodes Used in Lithium-Ion Batteries").

The collaboration with Superior Graphite (Chicago) continued with a focus to evaluate alternative graphitized carbons for the negative electrodes in Li-ion cells. Several meetings were held with the University of Michigan and Superior Graphite to identify the most-suitable physical properties to pursue in the manufacture

of improved carbons for higher charge/ discharge rate capability. Based on these discussions, the desired properties of the carbon include: (i) graphitized material, (ii) more-spherical particle morphology, (iii) final average particle size of 12 microns, and (iv) surface area of <15 m^2/g. Several samples were received from Superior Graphite for physical characterization. XRD analysis indicated the d(002) spacing is ~3.36 Å, typical of a highly graphitized material. Transmission electron microscopy (TEM) examination suggests a preponderance of 2-dimensional structure (*i.e.*, flake-like) rather than the desired 3-dimensional structure (*i.e.*, spherical). Discussions are in progress with Superior Graphite to evaluate their processing method.

A collaborative study was undertaken with HydroQuebec (HQ) to investigate the properties of mesocarbon microbeads (MCMBs) from Osaka Gas (Japan). The goal of this study was to investigate the properties of MCMBs after heat treatment (*i.e.*, 700, 1000, 1200, 1800, 2400 and 2750°C). Heat treatment was conducted in a graphitizing furnace, and physical characterization involving thermal analysis and TEM were performed at LBNL. The initial MCMBs, which are obtained by processing tar pitch at low temperatures, appeared to consist of mainly spherical particles (<30-micron diameter). Heat treatment in an inert atmosphere produced a substantial weight loss (~12%) and agglomeration of the particles. These results suggest that the initial MCMBs contained significant fractions of hydrogen and oxygen, indicative on a material that is not completely carbonized. In addition, heat treatment produced a significant change in particle morphology because of agglomeration. The electrochemical evaluation of these materials in Li-ion cells is currently underway at HQ.

The collaboration with the University of Michigan involves analysis of the role of carbon morphology on the irreversible capacity loss and electrolyte decomposition in Li-ion cells. Thermal analysis (TGA and DTA) involving air oxidation of carbons suggested that active sites are present which can be correlated to the crystallographic parameters, L_a and L_c, and the d(002) spacing. This finding was extended to determine the relationship between active sites on carbon and their role in catalyzing electrolyte decomposition leading to irreversible capacity loss (ICL). Electrochemical data from this study with graphitizable carbons and from published literature were analyzed to determine the relationship between the physical properties of carbon and the irreversible capacity loss during the initial charge/discharge cycles. Figure 1 shows the relationship between the ICL and L_a for carbons examined in this study and from other research groups. Despite the scatter in the plot, the trend shows that ICL is inversely proportional to L_a. Based on this analysis, we conclude that the active surface area, and not the total BET surface area, has an influence on the irreversible capacity loss of carbons for Li-ion batteries. This conclusion suggests that the carbon surface structure has a significant role in catalyzing electrolyte decomposition.

PUBLICATIONS

F. Kong, J. Kim, X. Song, M. Inaba, K. Kinoshita and F. McLarnon, "Exploratory Studies of the Carbon/Nonaqueous Electrolyte Interface by Electrochemical and *In Situ* Ellipsometry Measurements," *Electrochem. and Solid-State Lett.*, **1**, 39 (1998).

J. Kim, F. Kong, X.Y. Song, M. Inaba, K. Kinoshita and F. McLarnon, "Studies of the Carbon/Nonaqueous Electrolyte Interface by Electrochemistry, *In Situ* Ellipsometry and Impedance Spectroscopy," *193rd Meeting of the Electrochemical Society*, San Diego, CA, May 3-8, 1998.

T.D. Tran, D.J. Derwin, P. Zaleski, X. Song and K. Kinoshita, "Effects of Heat Treatment and Morphology of Petroleum Cokes on Lithium Intercalation," *193rd Meeting of the Electrochemical Society*, San Diego, CA, May 3-8, 1998.

G. Nazri, B. Yebka, M. Nazri, D. Curtis, K. Kinoshita and D. Derwin, "Safety and Reactivity of Carbonaceous Anode in Lithium Battery Technology," *193rd*

Meeting of the Electrochemical Society, San Diego, CA, May 3-8, 1998.

T.D. Tran, D.J. Derwin, P. Zaleski, X. Song and K. Kinoshita, "Lithium Intercalation Studies of Petroleum Cokes of Different Morphologies," *9th International Meeting on Lithium Batteries*, Edinburgh, UK, July 12-17, 1998.

T.D. Tran and K. Kinoshita, "Carbon for Supercapacitors and Li-Ion Batteries in EVs," *194th Meeting of The Electrochemical Society*, Boston, MA, November 1-6, 1998.

M. Inaba, R. Kostecki, K. Kinoshita and F. McLarnon, "Ti-, Zr-, Nb- and Mo-doped Lithium Manganese Oxide Positive Electrodes," *194th Meeting of The Electrochemical Society*, Boston, MA, November 1-6, 1998.

T.D. Tran, X. Song and K. Kinoshita, "Investigation of Lithiated Carbons by Transmission Electron Microscopy and X-Ray Diffraction Analysis," *Materials Research Society Fall Meeting*, Boston, MA, November 30 –December 4, 1998.

G. Nazri, B. Yebka, M. Nazri, D. Curtis, K. Kinoshita and D. Derwin, "Safety and Reactivity of Carbonaceous Anode in Lithium-Ion Batteries," *Materials Research Society Fall Meeting*, Boston, MA, November 30 –December 4, 1998.

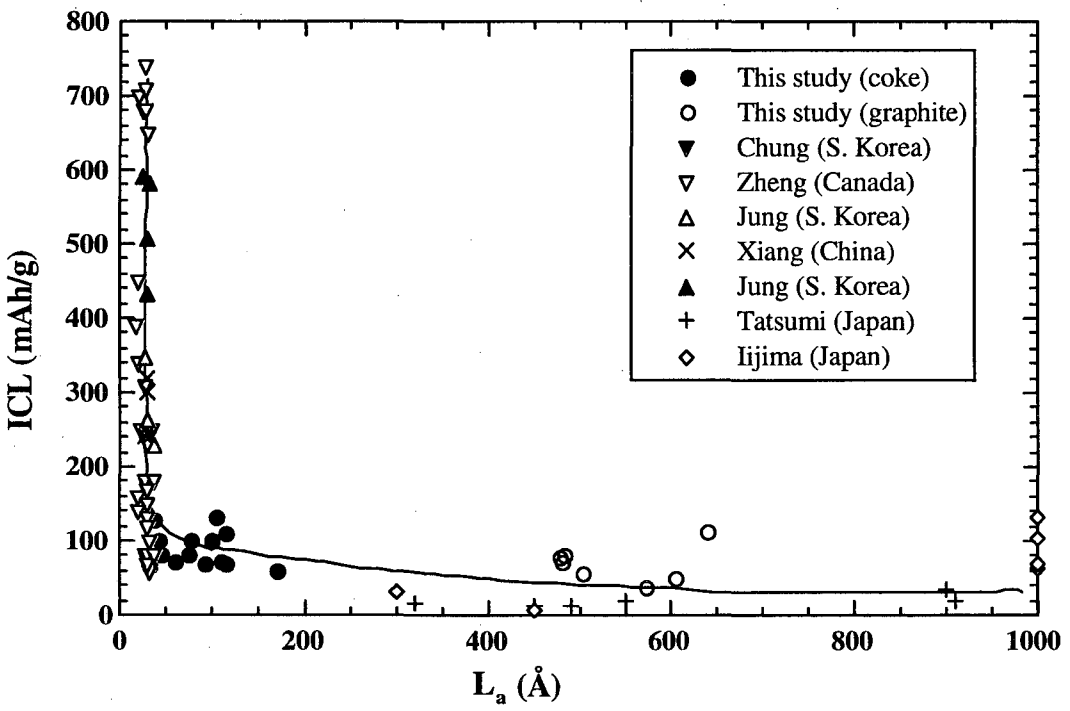

Figure 1. Composite plot of ICL *vs.* L_a for different types of carbon electrodes. Line indicates trend of the data.

Fabrication and Testing of Carbon Electrodes as Lithium-Intercalation Anodes

Tri D. Tran
L-282, Lawrence Livermore National Laboratory, P.O. Box 808, Livermore CA 94550
(925) 422-0915; fax: (925) 424-3281; e-mail: tran4@llnl.gov

Objectives

- Evaluate the performance of carbonaceous materials as hosts for Li-intercalation negative electrodes.
- Develop reversible Li-intercalation negative electrodes for advanced rechargeable Li-ion cells.

Approach

- Fabricate electrodes from various commercial carbons and graphites and evaluate in small Li-ion cells.
- Correlate electrode performance (*i.e.*, capacity, irreversible capacity) with carbon structure and properties in collaboration with LBNL.

Accomplishments

- The Li intercalation capacity of Santa Maria coke (x = 0.83) was found to be among the highest observed for untreated coke materials.

Future Direction

- Project is complete.

Several types of heat-treated cokes from Superior Graphite Company were investigated as electrode materials for Li^+ intercalation. The cokes include fluid coke, pitch coke, Santa Maria coke, electrode coke and nipple coke. These commercial cokes are generally heat treated (calcined) to a maximum temperature of about 1400°C to remove volatile components. The electrodes containing these cokes were prepared according to a standard procedure that uses pyrolyzed phenolic resin as the binder. The electrolyte is 0.5 M $LiN(CF_3SO_2)_2$, (3M Corp) in a 50:50 mixture of ethylene carbonate and dimethyl carbonate (Grant Chemical). Intercalation experiments were carried out at the C/24 rate using 3-electrode set-ups with Li foils as both counter and reference electrodes.

The cokes were milled and then sieved to average particle sizes of 10-25 μm. The air-milling technique and the particle morphologies allow for preparation of rather smooth surfaces resulting in low-surface-area powders. The reversible Li intercalation capacities of these cokes are in the range of 179 to 310 mAh/g, corresponding to x values of 0.48 to 0.83 (in Li_xC_6). The reversible capacity for Santa Maria cokes is considerably larger than that for a typical coke. The voltage profiles of all materials show amorphous-like behavior with gradual changes in voltage as the intercalation/deintercalation proceeds. TEMs of several samples showed disordered crystalline structures characteristic of cokes.

The cokes were heat treated at several temperatures between 1400 and ~2800°C to study the effect of heat treatment on the morphology, microstructure and subsequently the Li intercalation behavior. The fluid coke and the Santa Maria coke were selected because of their initial amorphous structure and their particle morphology, which are more globular in nature. In contrast, needle-like cokes such as nipple coke or electrode coke tend to have a preferred structural orientation. It is expected that more-spherical particles with graphitic structures derived from the fluid-type cokes can

lead to higher performances, particularly in terms of rate and particle size distribution. Successive heat treatment of the fluid coke at 1800 and 2300°C reduced the BET surface areas, and correspondingly reduced the irreversible capacity loss. The reversible capacity appears to pass through a minimum over this range but the performance for samples heat treated at 2300°C is only x = 0.55, well below that of graphitized needle-coke that had been treated at a similar temperature. The same trend was observed for another fluid-type coke (Santa Maria coke). The capacity for Santa Maria coke is among the highest observed for untreated coke materials. The potential profiles of these materials exhibit gradual changes with Li concentration, consistent with those from amorphous compounds. TEM observation shows evidence of ordered structure but the $d(002)_{spacing}$ of fluid coke heated to 2300°C (3.39 Å) suggests only partial graphitization.

PUBLICATIONS

T.D. Tran and K. Kinoshita, "Surface Modifications to Improve Performance of Carbon Lithium Intercalation Anodes," U.S. Patent Application submitted August 31, 1998

T.D. Tran, D.J. Derwin, P. Zaleski, X. Song and K. Kinoshita "Effects of Heat Treatment and Morphology of Petroleum Cokes on Lithium Intercalation," *193rd Meeting of the Electrochemical Society*, San Diego, CA, May 3-8, 1998.

T.D. Tran, D.J. Derwin, P. Zaleski, X. Song and K. Kinoshita, "Lithium Intercalation Studies of Petroleum Cokes of Different Morphologies," *9th International Meeting on Lithium Batteries*, Edinburgh, UK, July 12-17, 1998.

T.D. Tran and K. Kinoshita, "Carbon for Supercapacitors and Li-Ion Batteries in EVs," *194th Meeting of The Electrochemical Society*, Boston, MA, November 1-6, 1998.

T.D. Tran, X. Song and K. Kinoshita, "Investigation of Lithiated Carbons by Transmission Electron Microscopy and X-Ray Diffraction Analysis," *Materials Research Society Fall Meeting*, Boston, MA, November 30 –December 4, 1998.

Safety and Reactivity of Carbonaceous Anodes Used in Lithium-Ion Technology

*M. David Curtis and Gholam-Abbas Nazri**
Department of Chemistry, University of Michigan, Ann Arbor MI 48109-1055
**Physics and Physical Chemistry Department, GM Research and Development Center, Warren, MI 48090*
(734) 763-2132; fax: (734) 763-2307; e-mail: mdcurtis@umich.edu / gnazri@cmsa.gmr.com

Objective

- Evaluate safety, reactivity, and performances of various carbonaceous anodes for application in Li-ion battery.

Approach

- Design and fabricate electrodes and cells from various carbonaceous materials, and correlate electrochemical performances with structural parameters of carbon, in order to develop an accelerated screening strategy for anode materials.
- Evaluate reactivity of various carbonaceous electrodes toward electrolyte decomposition, gas generation, and surface film formation.
- Evaluate thermal stability and the nature of surface films formed on carbonaceous electrodes during operation of Li-ion batteries.

Accomplishments

- Novel electrode fabrication methods and cell designs have been used, which allow real-time analysis of gaseous species generated in Li-ion cells during charge-discharge cycles.
- Carbonaceous electrodes with fewer edge sites and extended basal plane are less reactive and safer to use in Li-ion technology.
- Carbonaceous electrodes with fewer surface functional groups, trapped and adsorbed impurities, and defect sites are less reactive and safer to be used in Li-ion systems. Functional groups and impurities can be removed at 1000°C. However, annealing of defect sites requires heat treatment up to 2800°C in the presence of soft carbon.
- A more-compact and more-stable surface film formed on a carbonaceous electrode when high initial charge-discharge rates were applied. The thickness of the surface film grows to a limit beyond which electron-tunneling process between the anode and electrolyte solvent molecules is no longer possible.

Future Directions

- Improve the safety of carbonaceous anode by surface modification and surface coating to avoid electrolyte decomposition and gas generation.
- Optimize the performance of carbonaceous anodes for high-power and high-energy applications.

The objective of this project is to evaluate the influence of carbon structural parameters toward electrolyte decomposition, gas generation, and surface film formation during initial charge-discharge cycling, in order to design a low-cost high-performance electrode for application in Li-ion batteries. Although carbonaceous anodes are very desirable for Li-ion technology, they have two major problems that require special research attention: 1) excessive electrolyte decomposition during the first lithiation process, and 2) the generation of gaseous species. The gases are detrimental to the performance of Li cells and they are considered a safety hazard, as the majority of the gaseous species formed are flammable; also some of the gases may also dissolve in organic electrolyte and participate in parasitic reactions.

A unique electrode fabrication method and cell have been designed to examine the reactivity of various carbonaceous electrodes toward electrolyte decomposition. Figure 2 shows the cell designed for *in situ* gas analysis.

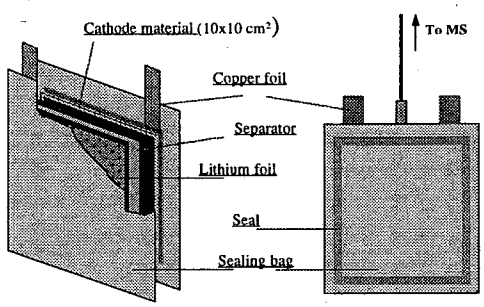

Figure 2. Schematic of cell used for gas analysis during charge-discharge cycling.

As shown in this work, the degree of graphitization of the carbonaceous electrode and structural parameters of graphite crystallites play critical roles in the safety of Li-ion batteries. A major effort was directed to understand the relationship between physicochemical properties of carbonaceous materials and their electrochemical performances. We found that the degree of crystallinity of the carbonaceous materials and the nature of electrolyte used are important factors for the electrochemical stability of Li-ion cells. The nature of gases generated during the initial Li insertion/extraction process

depends on electrolyte compositions and the nature of the carbon electrodes. We report results for a matrix of experiments, designed to study the electrochemical behavior of several combinations of carbonaceous electrodes in various carbonate-based electrolytes. Electrolytes and solvents used are given in Table 1.

Table 1. Solvents and electrolytes used

EC	DEC	DMC
EC- $LiPF_6$	DEC-EC	DMC-EC
EC-DEC-$LiPF_6$	DEC-$LiPF_6$	DMC-DEC
EC-DMC-$LiPF_6$	DEC-DMC-$LiPF_6$	DMC-$LiPF_6$
EC-PC-$LiPF_6$	DEC-PC-$LiPF_6$	DMC-PC-$LiPF_6$

We have also designed a unique diagnostic tool consisting of mass spectrometry and gas chromatography, to measure and identify gaseous species generated in Li-ion cells during charge-discharge cycling. The volume and composition of gaseous species generated on 18 different carbonaceous anodes in different electrolytes were recorded. We found two classes of gaseous species forming on carbonaceous electrodes; 1) the first class is usually generated before the electrolyte decomposition potential is reached, and is related to adsorbed and trapped impurities in carbon electrode, and 2) the second class includes gaseous species generated at about 0.8 volt *vs.* Li due to electrolyte decomposition; gas compositions are very sensitive to the electrolyte composition. The composition of major gaseous species detected during the initial lithiation of carbonaceous anodes in mixed-carbonate solvents are CH_4, C_2H_4, CO, and minimal amount of C_2H_6, H_2, and CO_2. However, when PC-containing electrolytes were used, the major gas components were C_3H_6 and CO. A significant amount of hydrogen was evolved when a trapped impurity such as moisture was present. We reported a complete table of gas compositions *vs.* the nature of graphites and electrolytes in our previous report. In order to cross check our results, we have now measured the H_2, CO and CO_2 amounts with specially designed gas chromatography equipped with sensitive columns for the detection of H_2, CO, CO_2.

In order to correlate the structural parameters of carbonaceous anodes to their performances we studied the morphology and crystal structure of variety of carbonaceous materials using SEM. The crystallite parameters and the degree of graphitization were measured by X-ray diffraction and Raman spectroscopy respectively. Surface area of carbonaceous electrode was measured using the BET technique. A correlation between the crystallite parameters in terms of degree of disorder and size of basal plane, L_a, *vs.* irreversible capacity loss and total volume of gas generated during the initial lithiation process is shown in Fig 3.

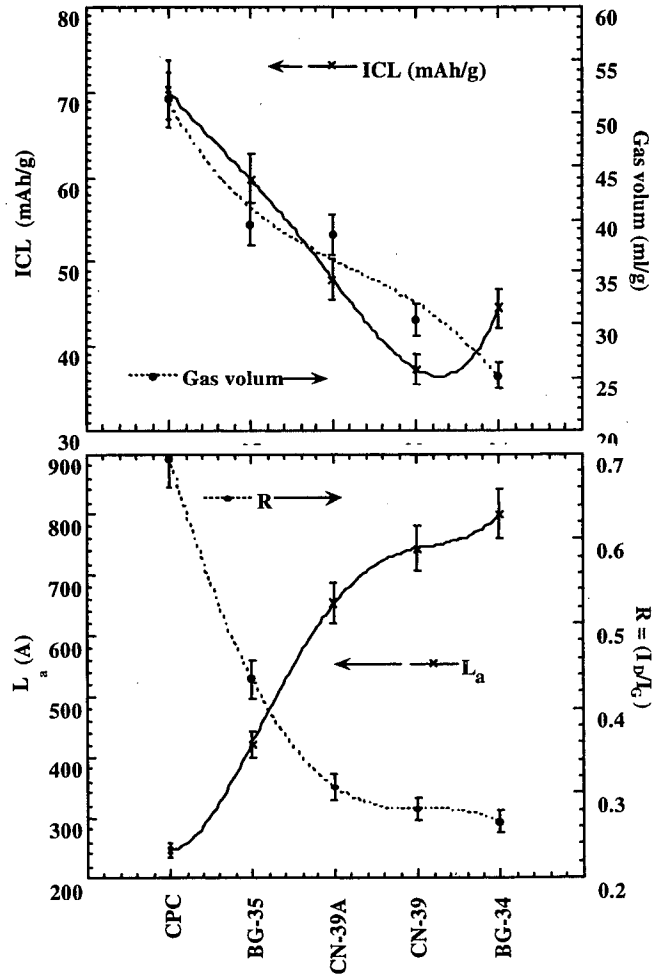

Figure 3. Correlation between structural parameters of carbonaceous anodes in terms of degree of disorder, R, and the size of basal plane, L_a, *vs.* irreversible capacity loss, and total volume of gas generated during initial lithiation process for several carbonaceous electrodes.

In order to develop a practical low-cost and high-performance anode, graphitic electrodes with low-edge surface area and a high degree of crystallinity should be considered. The graphitic materials provide significantly longer cycle life, higher volumetric energy density and a high-quality flat electrode potential profile (300-50 mV). The reactivity of the graphitic electrode can be significantly improved by adjusting the crystallite parameters, mainly by reducing the edge and defect sites containing sp^3 carbons and removing adsorbed and trapped impurities by heat treatment. Further modifications of graphitic electrodes require surface modification and surface coating which are the subject of our future investigations.

REFERENCES

G.A. Nazri, B. Yebka, M.D. Curtis, K. Kinoshita, D. Derwine, ECS, Proceedings Volume, Boston, Spring 1997. *194th Meeting of the Electrochemical Society*, Boston, MA, November 1-6, 1998.

G.A. Nazri, B. Yebka, M.D. Curtis, K. Kinoshita, D. Derwine, MRS Proceedings Volume 465, 1999.

Battery Materials: Structure and Characterization

James McBreen
Brookhaven National Laboratory, DAS-Bldg. 480, P.O. Box 5000, Upton NY 11973-5000
(516) 344-4513, fax: (516) 344-4071; e-mail: jmcbreen@bnl.gov

Objective

- Elucidate the molecular aspects of battery materials and processes by *in situ* high-resolution X-ray diffraction (XRD) and X-ray absorption (XAS).

Approach

- Apply *in situ* XRD and XAS to study low-cost Li_xNiO_2 and $Li_xMn_2O_4$ based cathodes, and tin-based composite oxide anodes.

Accomplishments

- *In situ* XRD studies were completed on Li_xNiO_2, Li_xCoO_2 and $Li_xNi_{1-y}Co_yO_2$ cathodes in rechargeable Li cells.
- *In situ* XAS was used to study the charge/discharge processes in a tin-based composite oxide anode ($SnB_{0.56}P_{0.4}Al_{0.4}O_{3.47}$).

Future Direction

- Utilize *in situ* XRD and XAS to study cycling behavior and failure mechanisms of Li intercalation electrodes.
- Develop diagnostic methods to study Li-ion battery materials that operate at high-rate charge and discharge.

The objective of this project is to elucidate the molecular aspects of materials and electrode processes in Li-ion batteries, and to use this information to develop electrode and electrolyte structures with low cost, good performance, and long life. Work during the year included both *in situ* high-resolution XRD and EXAFS studies on both anodes and cathodes for Li-ion batteries.

X-ray Absorption Studies of Tin-Based Composite Oxides (TCO): A tin-based composite oxide (TCO) material with a nominal

composition of $SnB_{0.56}P_{0.4}Al_{0.4}O_{3.47}$ was studied by *in situ* XAS. During the first charge cycle (Li insertion) the electrode accepted a charge of 708 mAh/g which corresponds to a Li/Sn ratio of 5.4. On the subsequent discharge the capacity was 424 mAh/g. Results obtained with the as-prepared material confirmed the amorphous nature of the TCO material and show that Sn in TCO is coordinated with three oxygen atoms at a distance of 2.12 A. Upon charging, Li initially interacts with the electrochemically active Sn-O center to form metallic Sn. The removal of oxygen from the Sn was quantitative. Upon further charge, Li reacts with Sn forming initially LiSn and then Li_7Sn_3 at a Li/Sn ratio of 5.4. Figure 4 shows the Fourier transform of the Sn K edge EXAFS during first charge (*i.e.*, Li insertion into the oxide).

The TCO material is amorphous and displays only a Sn-O interaction. Upon discharging (Li removal), metallic Sn is produced with a Sn-Sn distance intermediate to those of gray and white Sn. The coordination number is also low (<3). This indicates that Sn exists in a highly dispersed state in a matrix of Li_2O. After complete discharge there is no evidence of Sn-O interactions.

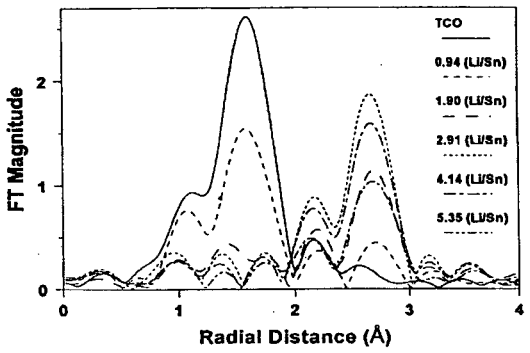

Figure 4. Fourier transform of the Sn K edge EXAFS during first charge of the TCO electrode.

X-ray Diffraction Studies (XRD) of $LiNiO_2$, $LiCoO_2$ and $LiNi_{1-x}Co_xO_2$: *In situ* XRD was carried out on cells with $LiNiO_2$, $LiCoO_2$ and $LiNi_{1-x}Co_xO_2$ (x = 0.1, 0.2, 0.3) cathodes that were charged at the C/10 rate. Cathodes were fabricated by casting a mixture of the cathode material ($LiNi_{1-x}Co_xO_2$, $LiCoO_2$, or $LiNiO_2$), acetylene black and a binder (PVdF) on an aluminum foil sheet. Disk electrodes (2.82 cm^2) were punched from the sheet and assembled in the cell with a Celgard separator and a Li foil anode. The electrolyte was 1 M $LiPF_6$ in solvent mixture of 1EC:3EMC. *In situ* XRD on $Li_{1-x}NiO_2$, during charge, in the 3.8 to 5.1 V region, revealed the formation of three hexagonal phases. In a similar voltage range $Li_{1-x}CoO_2$ showed three $CdCl_2$-type hexagonal phases and one CdI_2-type phase. Unlike reports of several other investigators, no monoclinic phases were observed. In the case of $Li_{1-x}NiO_2$ no phase change was detected until x = 0.4; whereas a phase change is detected in $Li_{1-x}CoO_2$ as early as x = 0.1. Substitution of even small amounts (x = 0.1) of Co in $Li_{1-x}NiO_2$ completely changes the phase behavior. The most obvious difference is that first phase change appears at x $\cong$ 0.1. Figure 5 shows a set of XRD spectra during charge of $LiNiO_2$.

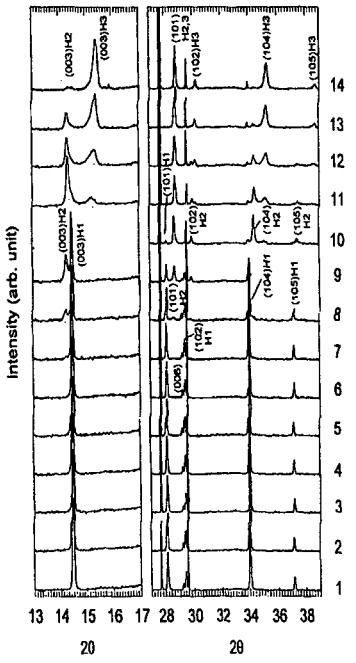

Figure 5. XRD spectra during charge of $LiNiO_2$. Scan 1 was recorded at the beginning of charge and scan 14 at the end of charge.

PUBLICATIONS

Y. Ein-Eli, S.H. Lu, W.F. Howard, S. Mukerjee, J. McBreen, J.T. Vaughey, and M.M. Thackeray, "$LiMn_{2-x}Cu_xO_4$ ($0.1 \leq x \leq .5$): A New Class of 5 V Cathode Materials for Li Batteries. I. Electrochemical, Structural and Spectroscopic Studies," *J. Electrochem. Soc.* **145**, 1238 (1998).

J. McBreen, S. Mukerjee and X.Q. Yang, *"In Situ* X-ray Studies of Battery and Fuel Cell Materials", *Synchrotron Radiation News,* **11(3)**, 18 (1998).

Y. Ein-Eli, S.H. Lu, M.A. Rzeznik, S. Mukerjee, X.Q. Yang, and J. McBreen, "$LiMn_{2-x}Cu_xO_4$ ($0.1 \leq x \leq 0.5$): A New Class of 5 V Cathode Materials for Li Batteries. II. In Situ Measurements," *J. Electrochem. Soc* **145**, 3383 (1998).

ELECTRODES FOR AQUEOUS ELECTROCHEMICAL CELLS

Electrodes are being developed to identify low-cost metal hydrides for MH/NiOOH cells and improved metal oxides for electrochemical capacitors.

Preparation of Improved, Low-Cost Metal Hydride Electrodes for Automotive Applications

James J. Reilly
Brookhaven National Laboratory, DAS-Bldg. 815, P.O. Box 5000, Upton NY 11973-5000
(516) 344-4502, fax: (516) 344-4071; e-mail: reilly@bnl.gov

Objectives

- Determine the properties and behavior of metal hydride electrodes with a view towards improving their lifetime and storage capacity, and decreasing their costs.
- Determine structure of complex AB_5 electrode alloys.
- Create a realistic mathematical model of the behavior of the MH_x electrode.

Approach

- Determine thermodynamic properties of alloy hydrides used in electrodes.
- Fabricate and test hydride electrodes.
- Employ and develop X-ray absorption spectroscopy (XAS) methods to determine the electronic structure, the local atomic environment and corrosion of alloy hydride electrode materials.
- Employ neutron diffraction to determine crystal structure.

Accomplishments

- Determined the crystal structure of $LaNi_{3.55}Co_{0.75}Mn_{0.4}Al_{.3}D_x$ and $La(Ni,Sn)_{5+x}$ alloys.
- Demonstrated that cobalt-free $La(Ni,Sn)_{5+x}$ electrodes have storage capacity and cycle life equal to or better than the commercial alloy $MmNi_{3.54}Co_{0.75}Al_{.3}Mn_{0.4}$

Future Direction

- Project was completed.

Crystal Structure of $La(^{58}Ni_{0.376}{}^{62}Ni_{0.624})_{3.55}Co_{0.75}Mn_{0.33}Al_{0.30}D_{4.73}$. The deuteride alloy, $La(^{58}Ni_{0.376}{}^{62}Ni_{0.624})_{3.55}Co_{0.75}Mn_{0.33}Al_{0.30}\ D_{4.73}$, was prepared and the hexagonal space group P6/mmm (#191) was used as a model to determine the crystal structure. The site preference of cobalt to occupy the 3g over the 2c sites was independently confirmed within two standard deviations from the value obtained for the uncharged alloy. Again, Al and Mn were determined to exclusively occupy the 3g sites. Four of the possible five deuterium sites were found to be occupied in the following order: the 12n site with n D atoms = 2.28(3) (D(3)), the 6m site with n = 1.70(3) (D(2)), the 12o site with n = 0.55(2) (D(1)) and the 4h site with n = 0.17(1) (D(4)). This leads to a stoichiometry of $AB_5D_{4.70}$ and corresponds to a lattice expansion of 17.6%. After the experiment the D content was determined *via* thermal decomposition to be 4.73 D atoms per formula unit, in excellent agreement with that obtained from the crystallographic refinement.

Crystal Structure of Non- Stoichiometric $La(Ni,Sn)_{5+x}$ Alloys. The $La(Ni,Sn)_{5+x}$ alloys were prepared in an arc furnace under inert gas and then annealed for three days at 1223 K. One alloy, E564, was obtained from a commercial vendor, Tribacher Auermet Produktions, GmbH. X-ray diffraction analysis indicated that the alloys were single phase. A total of six alloys (Table 1) were examined, four of which were $La(Ni,Sn)_{5+x}$ alloys. The composition is indicated by weight, the AB_5 stoichiometry normalized with respect to the rare earth component(s) and the structural formula as determined from the crystal structure. High-resolution X-ray powder diffraction patterns were collected at the National Synchrotron Light Source at BNL.

The X–ray Diffraction Pattern of $LaNi_{4.84}Sn_{0.32}$. E594 indicates that the sample is highly crystalline. The P6/mmm space group of stoichiometric $LaNi_5$ was preserved, as in the case of $La(Ni,Cu)_{5+x}$. The B(3,3) atomic displacement parameter indicates a large displacement of La along the *c* axis compared to the in-plane displacement. Aligning Ni dumbbells along the *c* axis in a random fashion will lead to this type of displacement parameter for the disordered dumbbell A-sites. The refinement also indicates that the electron density of the B-site in the basal plane (2c) can be fully accounted for by Ni occupation. Placing Sn on this site would lead to vacancies, which in view of the stoichiometry is not very likely. There is a substantial increase in the *c* axis and a decrease of the *a* axis of $LaNi_{4.84}Sn_{0.32}$ (E594) relative to the stoichiometric $LaNi_{4.7}Sn_{0.3}$ (E492). The contraction of the *a* axis indicates that the bigger Sn atom (atomic radius of 163 pm) does not occupy the basal plane 2c sites. The mid-plane 3g sites are occupied by Ni and all of the Sn. No indications of long-range superstructures could be found. The crystal structures of the other La-deficient alloys (E600, E601) were also determined and were found to similarly substitute Ni dumbbells on vacant A sites. The structure of the stoichiometric alloy, $LaNi_{4.7}Sn_{0.3}$ (E492) was also determined and Sn was found to exclusively occupy the 3g site.

Cycle Life of $La(Ni,Sn)_{5+x}$ Alloys. The $La(Ni,Sn)_{5+x}$ alloys were fabricated into electrodes containing 0.075 g of active material and cycled in an open cell containing 6 M KOH. The counter electrode was Pt and the reference electrode was Hg/HgO. The electrode was activated *in situ via* successive electrochemical charge and discharge cycles.

The results of the cycle tests are summarized in Table 2. The corrosion rate is based on the slope of the linear portion of the capacity *vs.* cycle life plots divided by Q_{max}. The number of hydrogen atoms/unit cell, n, is calculated from the maximum uptake, Q_{max}. Note that as the number of Ni dumbbell sites increase on the A sublattice, as indicated by the structural formulas, the corrosion rate decreases with only a small penalty in storage capacity. Finally when 4.45% of the A sites are occupied by Ni dumbbells the storage capacity exceeds that of the commercial alloy (E564) while the corrosion rate is less.

TABLE 1. ALLOY COMPOSITIONS

Element Ratio	Normalized Stoichiometry	Exp. #	Structural Formula
$La_{0.92}Ni_{4.60}Sn_{0.30}$	$LaNi_{5.00}Sn_{0.33}$	E600	$La_{0.9555}(Ni_{0.0445})_2Ni_{4.6885}Sn_{0.3115}$
$La_{0.95}Ni_{4.60}Sn_{0.30}$	$LaNi_{4.84}Sn_{0.32}$	E594	$La_{0.9781}(Ni_{0.0219})_2N_{i4.692}\ Sn_{0.308}$
$La_{0.965}Ni_{4.60}Sn_{0.30}$	$LaNi_{4.77}Sn_{0.31}$	E601	$La_{0.989}(Ni_{0.01097})_2Ni_{4.6925}Sn_{0.3075}$
$LaNi_{4.70}Sn_{0.30}$	$LaNi_{4.70}Sn_{0.30}$	E492	$LaNi_{4.70}Sn_{0.30}$
$MmNi_{3.55}Co_{0.75}Mn_{0.4}Al_{0.3*}$	$MmNi_{3.55}Co_{0.75}Mn_{0.4}Al_{0.3*}$	E564	$MmNi_{3.55}Co_{0.75}Mn_{0.4}Al_{0.3*}$
$LaNi_{4.3}Mn_{0.4}Al_{0.3}$	$LaNi_{4.3}Mn_{0.4}Al_{0.3}$	E132	$LaNi_{4.3}Mn_{0.4}Al_{0.3}$

*Mm refers to mischmetal with a composition 30 wt% La, 48% Ce, 15% Nd and 6% Pr.

TABLE 2. ELECTRODE PERFORMANCE

Structural Formula	Exp.#	Mol. Wt.	Q_{max} mAh/g	V_H, Å^3	H atoms unit cell	%•V/V	%Q Decay cycle	Stoich. x inAB_x
$La_{0.9555}\ (Ni_{0.0445})_2Ni_{4.6885}Sn_{0.3115}$	600	450	283		4.75		0.064	5.326
$MmNi_{3.55}Co_{0.75}Mn_{0.4}Al_{0.3}$	564	423	272	3.13	4.29	15.5	0.067	5.00
$La_{0.9781}(Ni_{0.0219})_2Ni_{4.692}Sn_{0.308}$	594	450	292	2.95*	4.89	16.1	0.081	5.157
$La_{0.989}(Ni_{0.01097})_2Ni_{4.6925}Sn_{0.3075}$	601	451	301		5.06		0.154	5.077
$LaNi_{4.7}Sn_{0.3}$	492	450	301	3.26	5.05	18.4	0.239	5.00
$LaNi_{4.3}Mn_{0.4}Al_{0.3}$	132	421	324	3.26	5.09	18.5	0.485	5.00

- Atomic volume of D in deuteride phase

PUBLICATIONS

T. Vogt, J.J. Reilly, J.R. Johnson, G.D. Adzic, E.A. Ticianelli, S. Mukerjee and J. McBreen, "High Cycle Life, Cobalt Free, AB_5 Metal Hydride Electrodes," in *Selected Battery Topics*, G. Halpert, M.L. Gopikanth, K.M. Abraham, W.R. Cieslak, W.A. Adams, eds., PV 98-15, Electrochemical Society, Pennington NJ, (1998).

E.A. Ticianelli, S. Mukerjee, J. McBreen, J.J. Reilly, J.R. Johnson and G.D. Adzic, "X-Ray Absorption Spectroscopy and Reaction Kinetic Studies of Yttrium Containing Metal Hydride Electrodes," in *Selected Battery Topics*, G. Halpert, M.L. Gopikanth, K.M. Abraham, W.R. Cieslak, W.A. Adams, eds., PV 98-15, Electrochemical Society, Pennington NJ, (1998). Boston, Massachusetts, Fall 1998.

T. Vogt, J.J. Reilly, J.R. Johnson, G.D. Adzic and J. McBreen, "Structure of Stoichiometric and Non-Stoichiometric AB_5 Type Alloys and Their Properties as Metal Hydride Electrodes," *Proc. of the Rare Earths Conference*, Fremantle, Australia, (1998).

Optimization of Metal Hydride Properties in MH/NiOOH Cells for Electric Vehicle Applications

Ralph E. White
Department of Chemical Engineering, University of South Carolina, Columbia, SC 29208
(803) 777-7314; fax: (803) 777-8265; e-mail: rew@sun.che.sc.edu

Objectives

- Optimize the alloy composition of metal hydride electrodes by microencapsulation of hydrogen-storage alloys.
- Develop a theoretical model to evaluate the equilibrium potential and the exchange current density as a function of state of charge of the electrode.
- Develop improved metal hydride electrodes for MH/NiOOH batteries.

Approach

- Prepare bare and Co-coated $LaNi_{4.27}Sn_{0.24}$ electrodes for determination of transport and electrochemical kinetic parameters.
- Determine the cycle lives of bare and electroless-coated alloys.

Accomplishments

- A ten-fold increase in cycle life and a 100% charge-discharge efficiency was achieved by the Co-P coating for $LaNi_{4.27}Sn_{0.24}$ alloys (250 cycles compared to 25 cycles at 0.3 C rate).
- No change in particle size for the Co-coated alloy is seen with cycling, consistent with impedance and laser measurements.

Future Direction

- Project was completed.

A theoretical model for the impedance of metal hydrides was developed that simulated the impedance response of a hydride electrode under diffusion and kinetic limitations. The effect of diffusion coefficient and particle size on the Nyquist plots was also studied, and it was found that decreasing the diffusion coefficient or increasing the particle size shifts the onset of the transition region to lower frequency values. Impedance data from the Co-plated $LaNi_{4.27}Sn_{0.24}$ electrode were obtained in the frequency range of 0.001 Hz to 10^{+5} Hz.

Nyquist plots of the Co-plated electrode revealed three regions at low frequencies, namely semi-infinite diffusion, transition and diffusion-limited regimes. The diffusion coefficient was calculated from the slope of the Nyquist plots in the transition region. It was found that the diffusion coefficient increases with an increase in the concentration of hydrogen in the particles. The decrease in diffusion coefficient with state-of-charge (SOC) was postulated to be due to the transformation from the β-phase to the α-phase at low SOC.

Electrochemical impedance spectroscopy (EIS) was used to study the effect of cycling on the alloy particle size. The impedance response of $LaNi_{4.27}Sn_{0.24}$ electrodes was obtained in the frequency range of 1 mHz to 100 kHz. The slopes of the transition regions in the impedance profile were used to calculate the particle size of the alloy. Pulverization behavior for the $LaNi_{4.27}Sn_{0.24}$ electrode was obtained by determining the particle size at the end of each discharge cycle.

More pulverization was observed with bigger particles and it gradually slowed down in an exponential manner. EIS was used to

determinate the particle size during cycling of Ni-MH batteries. Cycle-life studies on a $LaNi_{4.27}Sn_{0.24}$ alloy showed capacity decay even after the particle size stabilization, which shows that pulverization is not the only reason for capacity decay. X-ray studies showed the presence of a large amount of lanthanum oxides in the cycled alloy, indicating that alloy oxidation is an important factor in the capacity fade of metal hydrides.

The multi-step process for electroless plating of Co, Co-P, Ni, Ni-P and Co-Ni-P alloy was simplified to a one-step technique. A $LaNi_{4.27}Sn_{0.24}$ alloy was microencapsulated with Co and Co-Ni using this one-step deposition process, and characterization studies showed that Co has several advantages over other electroless coatings. The capacity fade in the bare alloy was absent and a constant capacity with cycling was obtained. The effect of deposition temperature and coating thickness on the alloy electrode performance was studied. Figure 6 shows the cycling behavior of the bare and Co-coated alloy. The performance of $LaNi_{4.27}Sn_{0.24}$ alloy mixed with Co is also presented for comparison. A ten-fold increase in cycle life is seen due to the Co microencapsulation. The capacity fade in the bare alloy is absent and a constant capacity with cycling is obtained. Further, thin Co films formed on the surface of the alloy enhance the overall capacity of the alloy significantly.

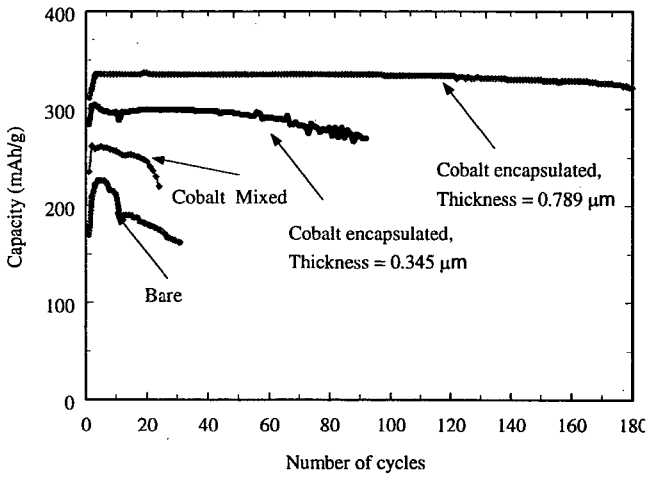

Figure 6. Cycle life studies on bare and Co-coated alloys.

PUBLICATIONS

B.S. Haran, B.N. Popov and R.E. White, "Theoretical Analysis of Metal Hydride Electrodes: Studies on Equilibrium Potential and Exchange Current Density," *J. Electrochem. Soc.* **145**, 4082 (1998).

B.S. Haran, B.N. Popov and R.E. White, "Determination of Hydrogen Diffusion Coefficient in Metal Hydrides by Impedance Spectroscopy," *J. of Power Sources,* **75**, 56 (1998).

B.S. Haran, B.N. Popov and R.E. White, "Studies on Electroless Cobalt Coatings for Microencapsulation of Hydrogen Storage Alloys," *J. Electrochem. Soc.* **145**, 3000 (1998).

B.N. Popov, G. Zheng, B.S. Haran and R.E. White, "Studies on Metal Hydride Electrodes with Different Weights and Binder Contents," accepted for publication in *J. Appl. Electrochemistry*, May (1998).

B.N. Popov, B.S. Haran and R.E. White, "Development of High Performance Metal Hydride Alloys by a Novel Electroless Plating Process," *193th Meeting of the Electrochemical Society*, San Diego, CA, May 3-8, 1998.

B.S. Haran, B.N. Popov, T. Cupolo and R.E. White, "Capacity Deterioration of Metal Hydride Alloys — Theoretical and Experimental Study," *193rd Meeting of the Electrochemical Society*, San Diego, CA, May 3-8, 1998.

A. Durairajan, B.S. Haran, B.N. Popov and R.E. White, "Studies on Hydrogen Diffusion in Metal Hydrides Using Impedance Spectroscopy," *194th Meeting of the Electrochemical Society*, Boston, MA, November 1-6, 1998.

A. Durairajan, B.S. Haran, B.N. Popov and R.E. R.E. White, "Development of High Performance Metal Hydride Alloys by Cobalt Microencapsulation," Proceedings of the Symposium on *Batteries for the 21st Century, 194th Meeting of the Electrochemical Society*, Boston, MA, November 1-6, 1998.

Microstructural Modeling of Highly Porous MH/NiOOH Battery Substrates

Ann Marie Sastry
Department of Mechanical Engineering and Applied Mechanics, The University of Michigan, Ann Arbor, MI 48109-2125
(313) 764-3061; fax: (313) 747-3170; e-mail: amsastry@engin.umich.edu

Objectives

- Develop stochastic geometry models for key morphologies of Li-ion electrode materials, to map connectivity of these microstructures over useful ranges of manufactured materials.
- Identify failure modes in cycled Li-ion and metal hydride/NiOOH cells and to understand the unique physical load mechanisms in negative-electrode substrate materials.
- Validate modeling efforts with electrochemical experiments, employing post-mortem investigations of material properties.

Approach

- Perform transport and mechanics simulations on stochastic geometry models for key morphologies of Li-ion electrode materials, including whiskers (~1 μm), fibers (~10 μm) and spheroidal particles (<10 μm) based on carbonaceous materials.
- Evaluate physical degradation of electrode materials with simulations using the stochastic 1D and 2D (finite element) models.
- Characterize damage progression through continued simulations, testing the validity of numerical approaches.

Accomplishments

- Identified ranges of applicability of a novel stochastic network generation technique compared with full-field finite-element solutions.
- Identified corrosion effects on material morphology by image analysis, and by mechanical and transport (electrical resistivity) testing of substrates.
- Refined damage simulations and validated experimentally the degradation hypothesis of mass transfer from particle to fiber morphology.

Future Directions

- Continue investigation of scale effects in simulation of mechanical damage and transport behavior in random networks.
- Conduct full-scale cell testing of Li-ion cells to assess to benchmark theoretical results from damage analysis.
- Develop new standards for cell testing to better assess electrode performance.

The objective is to develop predictive capability for the electrochemical performance of Li-ion and MH/NiOOH cells. The MH/NiOOH substrate materials have been completely characterized experimentally. Simulations based on the evolution hypothesis

depicted schematically in Fig. 7 have now been validated with experimental data. Good correlations were found from the simulations of electrical resistivity (Figs. 8 and 9). These simulation results demonstrated the utility of the stochastic network approach in both characterizing key morphological changes in substrates, and in suggesting design guidelines in the manufacture of superior materials. The hypothesis that corrosion and electrodeposition cause changes in substrate architecture was demonstrated to be valid qualitatively and quantitatively, and the models showed that these changes could be tractably represented by the methods developed.

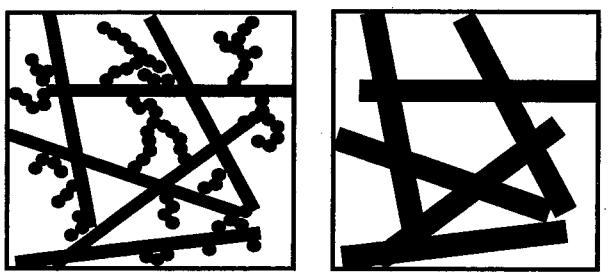

Figure 7. Evolution hypothesis for morphology of the positive plate, Ni/MH cells. Small Ni particles in the as-received material (a), which are thought to form an interconnected network with the fibers, are consumed in the electrochemical reaction and redeposited on the substrate (b).

Simulations also showed that rigorous bounds on behavior of fibrous media do not provide narrow-enough predictions of properties to allow design of substrates. Indeed, the stochastically arranged networks often fail to "percolate" for the technologically important case of very low volume fractions. Particularly in this regime, variance in both mechanical and transport properties is large, and the average is well below the upper bound. This has important implications where particles represent a significant portion of the material. These are the subjects of ongoing study.

Implications for Design of Substrates. Although compression of cells could eventually be eliminated with improved materials design, it is a commonly performed step to assure good transport over cycle life. Thus, material compression must be taken into account in design for conductivity. Also, the consumption and redeposition of particle mass in the cell causes very significant changes in the networks modeled. Doubling of aspect ratios of fibers has important consequences for transport properties; indeed, these morphological changes alone explain much of the reduction in conductivity measured experimentally. In essence, one must design for minimum conductivity in the post-cycled condition if substrates comprised of mixtures of fibers and particles are to be used. Further corrosion of the substrates is possible in more-aggressive cycling conditions and after prolonged cycling. The best strategy in modeling, however, is probably to separate electrodeposition modeling from the network behavior, thus carrying out design in two steps: first, assessing the likely changes in architecture during cycling, and second, modeling the conductivity of the final microstructure to determine minimum requirements on mass (volume). Simulations here show that the second step can be performed with excellent accuracy, and which are guided by experiments that deliver estimates for the determination of the microstructure.

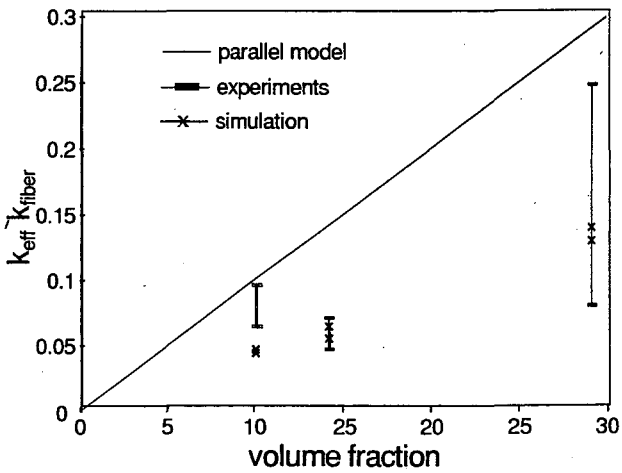

Figure 8. Simulations *vs.* experimental data. Resistivities of compressed materials *vs.* upper bound predictions and simulation results, for each material type (10, 14 and 29% volume fractions).

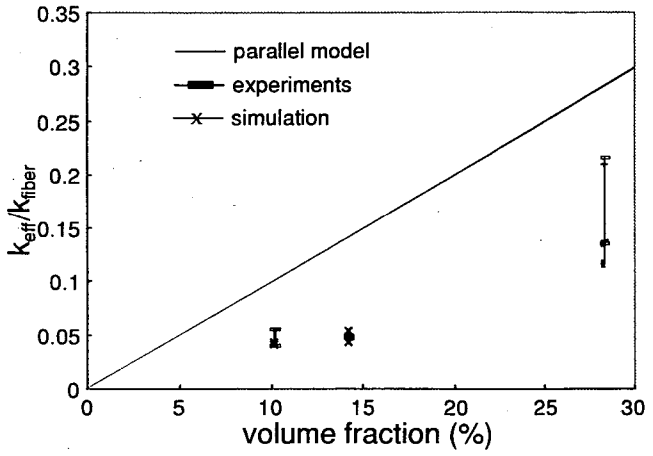

Figure 9. Simulations *vs.* experimental data. Resistivities of post-cycled materials *vs.* upper-bound predictions and simulation results, for each material type (10, 14 and 29% volume fractions).

The mechanical properties and models serve as "proof tests" of material evolution; they also indirectly address the matter of swelling. The 2-D simulations showed that bond stiffness must be quite low to explain the observed behavior, in the absence of plasticity in the model. Experimental evidence suggests very little overall permanent deformation of materials after cycling, motivating the elastic models, but displacements and rotations can be locally high in stochastic systems. The 3-D problem of material resistance to failure in transverse planes (*i.e.*, loss of conductivity of the positive plate due to transverse failures) must incorporate observations and simulations of the bond behavior in the plane. It is probably reasonable to assume that bonds behave much the same way, regardless of location, but the long beam sections which span the thickness of the materials would inherently offer much different balances of loads in bending, torsion and tension than the shorter beams in the plane of the networks studied, necessitating fully 3-D simulations for those materials.

The comparisons of micromechanical models and experimental data have produced good agreement for the materials studied. Results point to use of higher-aspect-ratio fibers for use in substrates, with modeling also necessary to account for structural changes during cycling.

PUBLICATIONS

A.M. Sastry, S.B. Choi and X. Cheng, "Damage in Composite NiMH Positive Electrodes," *ASME J. Engin Mats. and Tech.* **120**, 280-283, (1998).

A.M. Sastry, X. Cheng and C.W. Wang, "Mechanics of Stochastic Fibrous Networks," *J. of Thermoplastic Composite Mats.* **30**, 288-296, (1998).

C.W. Wang, X. Cheng and A.M. Sastry, "Failure of Stochastic Fibrous Networks," Proceeding of the *13th Annual Technical Conference of the American Society for Composites,* Baltimore, MD, September 21-23, 1998.

COMPONENTS FOR AMBIENT-TEMPERATURE NONAQUEOUS CELLS

Metal/electrolyte combinations that improve the rechargeability of ambient-temperature, nonaqueous cells are under investigation.

Novel Lithium/Polymer-Electrolyte Cells

Elton J. Cairns and Frank R. McLarnon
90-1142, Lawrence Berkeley National Laboratory, Berkeley CA 94720
(510) 486-4636, fax: (510) 486-4260

Objectives

- Investigate the behavior of advanced electrode materials in high-performance rechargeable batteries, and develop means for improving their lifetime and performance.
- Improve the cycle life and utilization of the sulfur electrode in Li/polymer/S cells.
- Identify new electrode structures and compositions which will eliminate or minimize this fundamental mechanism of capacity loss of Li/MnO_2 cells

Approach

- Fabricate and test Li/polymer electrolyte/sulfur cells.
- Use a completely new approach to synthesize MnO_x and related materials for Li cells.

Accomplishments

- Greatly improved sulfur utilization at 60 C and room temperature were achieved, both in the range of 400 mAh/g S
- Novel aerogel $Li_xMn_yO_4$ powders with very high surface area have demonstrated specific capacities up to 175 mAh/g, but show significant capacity fading with cycling.

Future Directions

- Use *in situ* UV/VIS spectroscopy to determine the mechanism by which the sulfur electrode operates.
- Improve the performance of MnO_x, making use of post-test characterization to identify the structure of the active component.

Li/S Cells. Effort continues to develop a spectroelectrochemical cell to identify the products of Li/S cell reactions during galvanostatic cycling. The goal is to identify the cause(s) of the rapid capacity fade which is characteristic of this high-energy cell. Attempts to prepare LiAl negative electrodes by electro-alloying Li into an expanded Al mesh resulted in a brittle structure that either disintegrated into the electrolyte or punctured the polymer electrolyte and then shorted the cell. Negative electrodes prepared by electrodepositing Li onto a Ni grid were also unsuccessful because the Li either dissolved into the electrolyte or formed a grainy, highly reactive film that corroded before use. A cell sandwich with annular sulfur and Li foil electrodes is now used which allows the light beam to pass only through the polymer electrolyte. This cell design avoids the difficulty of preparing semi-transparent electrodes, and has allowed us to collect preliminary spectra. Galvanostatic studies on

Li/S cells indicated that the first (higher-voltage) plateau is retained longer and capacity fade is reduced by limiting discharges to ~25% of the theoretical cell capacity. These results suggest that during this stage of discharge, polysulfides are formed. The effects of other variables such as operating temperature and discharge/charge currents on cell lifetime were also studied, however no significant trends were identified for the limited ranges of these variables that were studied.

Li/S cells prepared with polyethylene-methylene oxide (PEMO) electrolyte were cycled at room temperature and at 60°C. Positive electrodes with 50% sulfur, 35% electrolyte and 15% carbon achieved a maximum utilization of 45%, or about 375 mAh/g-cathode at 60°C. The capacity faded fairly rapidly upon continued cycling to the lower voltage cutoff of 1.7 V vs. Li/Li^+. The capacity of 375 mAh/g-cathode is ~65% of the goal of 70% utilization at 60°C. Experiments are in progress to achieve a capacity goal of ~400 mAh/g-cathode at room temperature. This goal was recently met using a gel electrolyte consisting of thermally cross-linked fumed silica and butyl methacrylate as the mechanical backbone, with PEGDME as the plasticizer. The conductivity of this electrolyte at room temperature obtained by ac impedance measurements is $>10^{-3}$ S/cm^2, which is among the highest conductivities for a gel electrolyte that contains no carbonate-based plasticizer. The positive electrode of this Li/S cell contains 50% sulfur, 30% PEGDME + salt, 5% PEO and 15% carbon.

Novel Cathode Materials. Aerogel $Li_xMn_yO_4$ powders with very high surface area were prepared. Initial tests showed good performance with a first discharge capacity of 175 mAh/g, however severe capacity fading accompanied cycling. Some of the capacity fading was attributed to the presence of water in the aerogel structure. Using a uniquely designed drying tube and a new electrode fabrication method, water has been removed from the aerogel powder and reabsorption of water was prevented. The new electrodes exhibit a lower first discharge capacity of 150 mAh/g, but the rate of capacity fade during cycling decreased. Several electrode fabrication techniques using different orders of mixing the electrode components, current collectors, and drying temperature were evaluated to maximize the utilization of the active material. No major improvements were observed using the various techniques, and the cause of the severe capacity fade remains under investigation. Elemental analysis will be used to determine the exact composition of the aerogel, and the manganese oxidation state of the aerogel will be determined using an iron sulfate chemical titration technique.

Other compositions of lithium metal oxide aerogel materials will be synthesized using sol-gel methods followed by CO_2 supercritical drying. The aerogel powders will be characterized by XRD to verify an amorphous structure, thermogravimetric analysis to determine dryness and thermal stability, and SEM to measure the micropore size. The new material will be used to produce test cells for performance and cycle-life evaluation.

PUBLICATION AND PRESENTATION

T.C. Adler, F.R. McLarnon and E.J. Cairns, "Investigations of a New Family of Alkaline-Fluoride-Carbonate Electrolytes for Zinc/Nickel Oxide Cells," *Ind. Eng. Chem. Research*, **37**, 3237-41 (1998).

D. Marmorstein, H.-J. Ahn, K. Striebel, F. McLarnon and E.J Cairns, "Lithium/Polymer/Sulfur Cells," *194th Meeting of the Electrochemical Society*, Boston, MA, November 1-6, 1998.

New Cathode Materials

M. Stanley Whittingham
Chemistry and Materials Research Center, State University of New York at Binghamton, Binghamton, NY 13902-6000
(607) 777-4623, fax: (607) 777-4623; e-mail: stanwhit@binghamton.edu

Objectives

- Synthesize and evaluate oxides of manganese oxides for alkali-metal intercalation electrodes. Complete work on vanadium oxides.
- Identify new intercalation compounds for positive electrodes in advanced nonaqueous secondary batteries.

Approach

- Synthesize metal oxides that have an appropriate crystallographic structure to permit facile intercalation of Li ions.
- Characterize the metal oxide structures by XRD analysis and evaluate materials in electrochemical cells.

Accomplishments

- Synthesized a range of transition metal substituted layered manganese oxides: $A_xM_yMnO_2$ (A = Li, Na, K and M = Fe, Co, Ni) and showed that the cobalt compounds gave the best cycling results.
- Identified several new phases of vanadium-stabilized manganese oxides.
- Measured electrochemical cycling of the new phase $H_2V_3O_8$, and found good cyclability.

Future Directions

- Continue synthesis and electrochemical studies of manganese oxides.
- Use more-stable crystalline lattices.

The objective of this project is to synthesize and evaluate first-row transition metal oxides for Li intercalation electrodes in advanced nonaqueous rechargeable batteries. Mild hydrothermal techniques are being used for the synthesis, and in cases where the highest oxidation states are not obtained, other methods will be explored to drive the transition metal to its highest oxidation state. Manganese oxides are particularly attractive as the cathode, and means of stabilizing the layered manganese dioxide structure are being explored.

An attempt to incorporate nickel, in place of an alkali ion, into layered manganese dioxide by the hydrothermal decomposition of TMA•MnO_4 in the presence of Ni salts led to the formation of a totally new structure with the formula $HNiMnO_3$ rather than a simple layered manganate Ni_yMnO_2. Unfortunately, reaction in an electrochemical cell is very slow. Thus, we synthesized a range of layered manganates, $A_xM_yMnO_2$, (A = Li, Na, K and M = Fe, Co, Ni) in the temperature range 700-950°C. Initially Ni was chosen to "alloy" with Mn, as the total electron count would be more like that of $LiCoO_2$. The reactants, Na_2CO_3, Mn_2CO_3 and NiO were reacted to give the expected hexagonal structure with a=2.876(6) Å and c=11.16(2) Å. The compound was ion-exchanged to the Li form as follows:

$$NaMn_{2/3}Ni_{1/3}O_2 \xrightarrow[\text{hexanol, 160°C}]{\text{LiBr}} LiMn_{2/3}Ni_{1/3}O_2$$

The electrochemical cycling of $NaMn_{2/3}Ni_{1/3}O_2$ is shown in Fig. 10 (left). The compound must be charged first as little Li is incorporated during a first discharge. Essentially all of the Na was removed below 5 V, and 0.8 Li was incorporated on the subsequent discharge. However, only 0.6 of that Li could be removed and capacity fading was rapid. Thus, a second sample was first ion-exchanged with Li to give $(Li_{1-y}Na_y)Mn_{2/3}Ni_{1/3}O_2$ and then cycled electrochemically. The results are shown in Fig. 10 (right); 0.55 Li was removed below 4.6 V, and the subsequent discharge and charge cycle are shown.

X-ray analysis indicates that NiO is present as an impurity. In contrast, the Co- and Fe-substituted compounds appear to be CoO- and FeO-free for the composition $K_yCo_{0.1}Mn_{0.9}O_2$. Our present work therefore targets those materials, with particular emphasis on the K compound because K^+ ions are preferable to Na^+ or Li^+ ions in the lattice. Electrochemical data collection is now underway on these materials.

The pure trivalent manganese compounds were found to have a high resistivity, typically 10^5 to 10^7 ohm-cm at room temperature, similar to MnOOH in dry cells. In contrast, Co doping of the Mn sites such as in $K_yCo_{0.1}Mn_{0.9}O_2$ drops the resistivity by two orders of magnitude.

Summary of Vanadium Oxide Compounds. Studies of vanadium oxide compounds were completed. The tunnel/layered compound $H_2V_3O_8$ was obtained by solvothermal synthesis in acetic acid. Its structure and electrochemical behavior is shown in Fig. 11. The repeatability of the discharge curves suggests that the structure is maintained during cycling. The synthesis of a number of vanadium-substituted manganese oxides is underway and an interesting new material appears to have been formed that has a hexagonal structure and has an open pipe morphology.

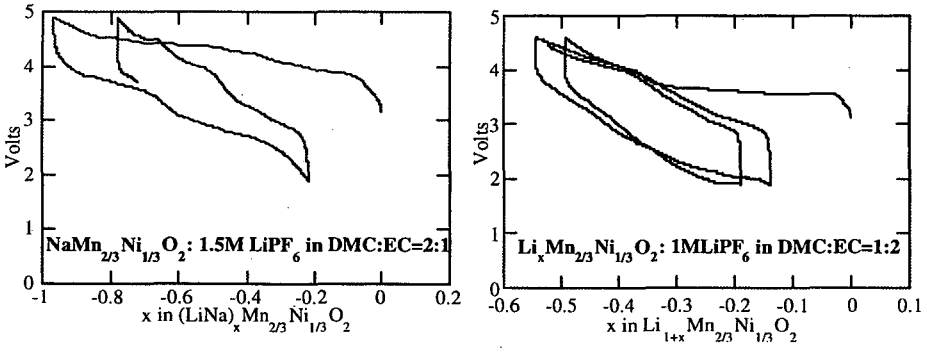

Figure 10. The electrochemical cycling of the cell made by using 80% $(Na,Li)Mn_{2/3}Ni_{1/3}O_2$, 10% carbon black and 10% Teflon powder as cathode, Li metal ribbon as anode and $LiAsF_6$ in PC:DMC as electrolyte.

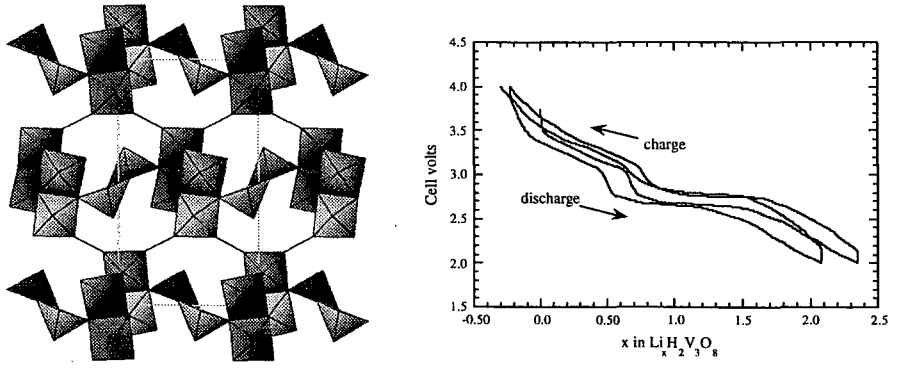

Figure 11. Structure of $H_2V_3O_8$ (left) and electrochemical behavior (right).

PUBLICATIONS

T.A. Chirayil, P.Y. Zavalij, M.S. Whittingham, "Hydrothermal Synthesis of Vanadium Oxides," *Chem Mater.* **10**, 2629-2640 (1998).

R. Chen, P.Y. Zavalij, M.S. Whittingham, "The Hydrothermal Synthesis and Characterization of New Organically Templated Layered Vanadium Oxides by Methylamine," *Mat. Res. Soc. Proc.,* **497**, 173-180 (1998).

M.S. Whittingham, "The Relationship Between Structure and Cell Properties of the Cathode for Lithium Batteries," in *Lithium Batteries,* O. Yamamoto and M. Wakihara, eds., Kodansha, Tokyo, Japan (1998).

F. Zhang, P.Y. Zavalij and M.S. Whittingham, "Hydrothermal Synthesis and Characterization of a Series of Novel Zinc Vanadium Oxides as Cathode Materials," Mat. Res. Soc. Proc., **496**, 367-372 (1998).

Solid Electrolytes

Lutgard C. De Jonghe
62-203, Lawrence Berkeley National Laboratory, Berkeley CA 94720
(510) 486-6138, fax: (510) 486-4881; e-mail: lcdejonghe@lbl.gov

Objectives

- Develop highly conductive novel composite electrolytes that combine the best features of single-ion conductors with those of polymer or gelled electrolytes, and to understand their transport properties.
- Develop high-capacity, robust MnO_2 cathode materials for rechargeable Li and Li-ion cells based on the $Na_{0.44}MnO_2$ tunnel structure.

Approach

- Develop methods for understanding transport properties of complex electrolyte systems.
- Fabricate composite electrolytes containing a single-ion conducting component with a conventional polymer or gelled component
- Synthesize and characterize MnO_2 based on the $Na_{0.44}MnO_2$ structure to achieve improved reversible capacity, cycle life and resistance to abuse (*e.g.*, overcharge and overdischarge) in Li-polymer and Li-ion cells.

Accomplishments

- Characterized transport properties of PPO-$LiCF_3SO_3$ and PPO-$LiN(CF_3SO_2)_2$ polymer electrolyte systems.
- Designed cell to determine effect of electro-osmotic solvent drag in gelled, liquid or composite electrolytes.
- Demonstrated reversible capacity of 90-100 mAh/g (approximately half the theoretical capacity) for Li_xMnO_2 based on the $Na_{0.44}MnO_2$ structure, at voltages compatible in metallic Li/polymer configurations.
- Demonstrated stability of Li_xMnO_2 based on the $Na_{0.44}MnO_2$ structure between 1-5 V *vs.* Li.

Future Directions

- Project was redirected to develop robust tunnel-containing manganese oxide structures for cathode materials.
- Improve cycle life and rechargeable capacity (≥200 mAh/g theoretical capacity) of MnO_2 by electrochemical and structural characterization.
- Demonstrate an increased capacity at ~3 V to at least 150 mAh/g by doping manganese oxide with titanium.

The initial goal for the project was to fabricate novel composite electrolytes that combine the advantages of single-ion conductors with that of gelled or polymer electrolytes. Another goal was to develop new methods to determine transport properties of gelled and composite electrolytes. This program was redirected in the fall of 1998, and the new emphasis is to develop novel, high-capacity electrodes based on tunnel-containing manganese oxides for rechargeable Li and Li-ion batteries.

Two studies of transport property of binary salt/polymer systems were completed in collaboration with J. Kerr's group (Polymer Electrolyte Synthesis for High Power Batteries). Results on polypropylene oxide (PPO)-$LiCF_3SO_3$ and $Li(NCF_3SO_2)_2$ show that higher Li^+ transference numbers and conductivities are obtained when the latter salt is used. It has been recognized that, in addition to salt concentration gradients in polymer or gelled electrolytes that arise during passage of current, electro-osmotic solvent drag can also occur. In extreme cases, drying or flooding of cell components can occur, causing premature cell failure. Figure 12 shows a schematic representation of an experimental cell to quantify this phenomenon.

The device consists of two cell halves that are sealed with an O-ring seal. An HDPE-encapsulated plunger holds a stainless steel platform onto which the Li electrode is pressed, and electrical contact is made *via* tungsten wires embedded in the plungers. The electrodes can be placed up to 1-cm apart. The test membrane, which can be a gelled or composite polymer electrolyte or a separator material such as Celgard, is clamped into a threaded holder placed between the two electrodes. To prevent bubbles and to ensure complete wetting of the membrane, the device is vacuum-filled through either of the two fill valves. The device holds ~30 mL of electrolyte solution when filled. Most of the internal volume is occupied by the HDPE plungers, and the solution must flow around them. Two graduated capillary tubes are attached *via* Swagelok connectors, and a 1-mm distance on the capillary tube corresponds to 1.87×10^{-7} ml, so the device is very sensitive to volume changes. No metal except Li contacts the electrolyte solution and there are no bubbles or leaks observed when the cell is properly assembled.

The work in this laboratory was recently redirected towards a study of novel tunnel-containing MnO_2 based on the $Na_{0.44}MnO_2$ structure. Lithium ion-exchanged materials made from $Na_{0.44}MnO_2$ have a high degree of reversibility toward intercalation processes and they are resistant to degradation when over-charged or over-discharged. Furthermore, conversion to the thermodynamically favored spinel structure does not occur below about 400°C, nor does degradation occur upon cycling at elevated temperatures. $Na_{0.44}MnO_2$ has an unusual double tunnel structure, which can accommodate intercalation and de-intercalation of either Na or Li ions without undue stresses, rendering it extremely robust (Fig. 13) to overcharge and overdischarging. The present research is directed towards improving the voltage profile by doping to increase the capacity in the 3 V region (for Li batteries) or in the 4 V region (for Li-ion batteries).

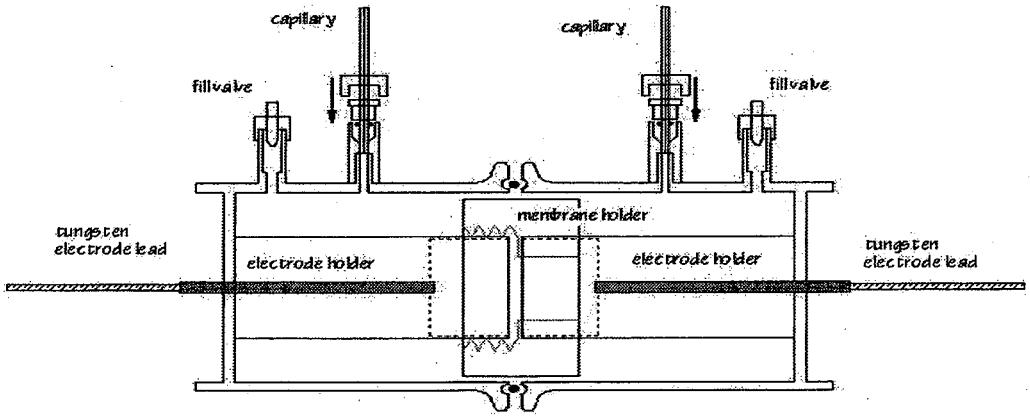

Figure 12. Cell set-up for electro-osmotic drag measurements.

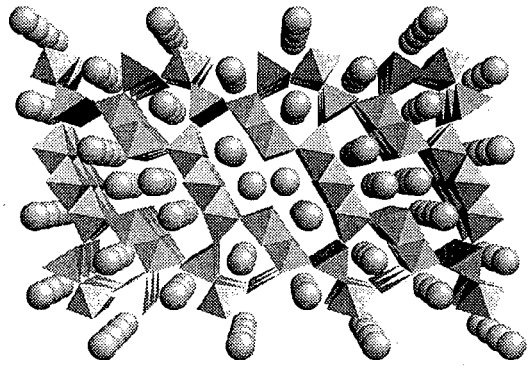

Figure 13. Structure of $Na_{0.44}MnO_2$, looking down the c-axis. The spheres represent sodium atoms or sites for Na atoms. In the as-made material, the sites in the small tunnels are fully occupied while the sites in the large S-shape tunnels are approximately half occupied.

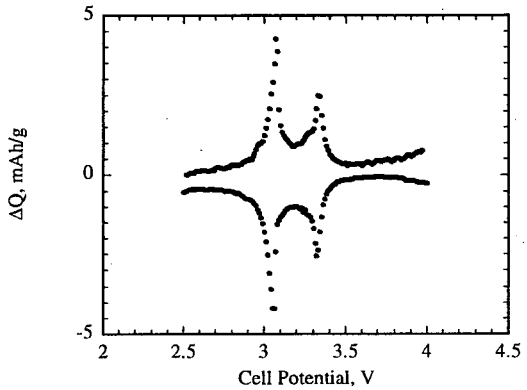

Figure 14. Differential capacity as a function of potential between 3.9 and 2.5 V for a Li/Li_xMnO_2 cell stepped 10 mV every four hours. The electrolyte is 1 M $LiPF_6$ in 1:1 EC/PC. The cell was charged prior to the experiment. The lower trace represents cell discharge and the upper trace cell charge.

No significant degradation of Li-exchanged $Na_{0.44}MnO_2$ cathodes occurs between 1 and 5 V *vs.* Li during slow cyclic voltammetry scans in cells with liquid electrolytes. The remarkable stability and reversibility of this material can be attributed to its unusual double tunnel structure (Fig. 13), which is flexible enough to undergo intercalation processes without stress, and requires substantial rearrangement to form a close-packed structure such as the spinel. Figure 14 shows the results of a stepped potential experiment on a Li_xMnO_2/Li cell with a liquid electrolyte, which illustrates the extraordinary reversibility of this material.

Evidence obtained in this laboratory suggests that it may be possible to insert more than 0.66 Li/Mn in the Na_xMnO_2 structure due to the smaller size of the Li ion; this implies that capacities above 200 mAh/g may be achievable. In practice, the capacity in Li-cell configurations varies with the degree of exchange, temperature, and voltage limits used. About 140 mAh/g is utilized in partially exchanged materials discharged between 3.7 and 2.5 V at 85°C in Li/polymer electrolyte cells. Completely exchanged materials exhibit less capacity and a higher average voltage between these limits, as well as having a smaller unit cell size than analogs containing residual Na.

The ECPS experiments show that Li intercalation and extraction processes between 3.9 and 2.5 V *vs.* Li are extremely reversible. Most of the capacity is located between about 2.9-3.4 V *vs.* Li and the voltage profile is gradually sloping in this region with several small plateaus. When charged past a composition of about $Li_{0.3}MnO_2$, the voltage rises steeply. At 3.9 V *vs.* Li, the composition is approximately $Li_{0.28}MnO_2$, corresponding to a capacity of ~85 mAh/g left in the structure.

Leaving residual Na in the structure, which increases the unit cell size, allows more capacity to be utilized below 3.7 V *vs.* Li in Li cells. Under normal cycling conditions below this voltage, further exchange is unlikely to occur for compositions containing ~0.14 Na/Mn, except at elevated temperatures. It is possible, however, that Na ions would be de-intercalated if the cell is charged above 4.2 V *vs.* Li, causing a decrease in unit cell size and lowered capacity in the normal operating range. Because cells in EV battery packs are susceptible to over-charging, this is undesirable. An alternative approach to increasing the capacity is to replace some of the Mn in the structure with a transition metal that is easier to oxidize, such as Ti.

So far, we have succeeded in synthesizing compounds in which 11, 22 and 55% of the Mn has been replaced with Ti. Both $Na_{0.44}MnO_2$ and $Na_{0.44}Ti_{0.55}Mn_{0.45}O_2$ belong to the same space group (*Pbam*), but the latter has a somewhat larger cell volume than the former (712 $Å^3$ compared to 680 $Å^3$). XRD studies indicate that $Na_{0.44}Ti_{0.11}Mn_{0.89}O_2$ and $Na_{0.44}Ti_{0.22}Mn_{0.78}O_2$ are isostructural, and have slightly larger unit cells than $Na_{0.44}MnO_2$. Provided that this size differential is maintained during Li-ion exchange, it is likely that there will be a beneficial effect on utilization at potentials practical for Li battery operation.

PUBLICATIONS

M.M. Doeff, P. Georen, J. Qiao, J. Kerr and L.C. De Jonghe, "Transport Properties of a High Molecular Weight Poly(propylene oxide)-$LiCF_3SO_3$ System," *193rd Meeting of the Electrochemical Society*, San Diego, CA, May 3-8, 1998. LBNL-42081

M.M. Doeff, J. Hou, J.B. Kerr, J. Qiao and M. Tian, "Synthesis and Testing of Comb-branch Polymers for Lithium Batteries and Electrochromic Windows," *193rd Meeting of the Electrochemical Society*, San Diego, CA, May 3-8, 1998.

M.M. Doeff and J. Reed, "Li Ion Conductors Based on Laponite/Poly(Ethylene Oxide) Composites," *Solid State Ionics*, **115**, 109 (1998).

A. Ferry, M.M. Doeff and L.C. De Jonghe, "Transport Property and Raman Spectroscopic Studies of the Polymer Electrolyte System $P(EO)_n$-NaTFSI," *J. Electrochem. Soc.* **145**, 1586 (1998).

A. Ferry, M.M. Doeff and L.C. De Jonghe, "Transport Property Measurements of Polymer Electrolytes," *Electrochim. Acta.* **43**, 1387 (1998).

T.J. Richardson, P.N. Ross, Jr. and M.M. Doeff, "XRD Studies of Lithium Insertion/Extraction in Cathodes Derived from $Na_{0.44}MnO_2$," *194th Meeting of The Electrochemical Society*, Boston, MA, November 1-6, 1998.

M.M. Doeff, P. Georen, J.B. Kerr, S. Sloop and L.C. De Jonghe, "Effect of Microphase Separation on the Measurement of Transport Properties of Polymer Electrolytes," *194th Meeting of The Electrochemical Society*, Boston, MA, November 1-6, 1998.

Polymer Electrolyte Synthesis for High-Power Batteries

John B. Kerr
62-203, Lawrence Berkeley National Laboratory, Berkeley, CA 94720
(510) 486-6279; fax: (510) 486-4995; e-mail: jbkerr@lbl.gov

Objectives

- Develop methods to prepare, purify and characterize polymer electrolyte materials.
- Measure Li-ion transference numbers in polymer electrolytes.
- Develop structure-function relationships involving polymer structure and (i) Li^+-ion transport through the bulk polymer and electrode interfaces, (ii) stability towards electrode materials in dynamic cycling and (iii) mechanical and thermal properties.

Approach

- Prepare comb-branch polymers (polyvinylether, polyacrylate ethers and polyepoxide ether) containing 2 to 8 ethylene oxide groups in the side chain.
- Prepare single-ion conductor materials by fixing anions to the side chains of the comb-branch polymers.
- Measure transference number by electrochemical methods and electrophoretic NMR.
- Assess polymer purity and stability towards Li metal by half-cell cycling, impedance spectroscopy and post-mortem chemical analysis.

Accomplishments

- Measurements on a variety of comb-branch and linear polymers containing segments of ethylene oxide units at least 5 units long show that the conductivity is the same regardless of the polymer architecture. The conductivity limit of 5×10^{-5} S/cm at 25°C was reached with ethylene oxide units as the solvating polymer structure.
- Thermal and transport property studies on Parel (high-MW PPO)/$Li(CF_3SO_2)_2N$ and amorphous PEO/ $Li(CF_3SO_2)_2N$ and $LiCF_3SO_3$ were completed.
- Polyelectrolytes with unit transference numbers were prepared and tested.

Future Directions

- Complete transport measurements of selected comb-branch polymers containing polyacrylate ethers, polyvinyl and polyepoxide ethers and a variety of salts.
- Prepare comb-branch polymers with pendant crown ether units of different ring size and flexibility of the crown ether units. Prepare single-ion conductor materials with practical conductivities and confirm predicted benefits of these materials.
- Develop methods to measure side reactions at electrodes and provide rate data to validate electrochemical system models designed to predict failure behavior of batteries.

Synthesis. Synthesis of vinyl-ether monomers using the Williamson reaction with diethyleneglycolvinyl ether and monomethyl ether of polyethylene glycol ethylchloride yielded a variety of chain lengths from 2 to 7 ethylene oxide units. Several initiation systems were employed to produce living polymer conditions. The non-stoichiometric $Et_{1.5}AlCl_{1.5}$ gave polymers with increased MW from those reported in the literature but the PDI ratio of 1.7-1.8 shows that the living polymer was not achieved. Attempts were made to increase the MW by using more-controlled conditions, varying the initiator/monomer ratios and the use of chain-extension agents. The structure of these agents influences the MW of the polymer and excess cross-linker leads to the formation of intractable rubbers. We could not produce high-molecular-weight polymers under living polymer conditions.

Polyepoxide ethers were successfully prepared by anionic initiation conditions and, polyacrylate ethers were formed under radical conditions. It was noted that the radical conditions could not be completely quenched and uncontrolled cross-linking continued to occur indefinitely leading to intractable rubbers. An alternative method of *in situ* cross-linking was developed which provides self-standing polymer films with excellent mechanical properties.

Characterization of Comb-branch (CB) and Comb-branch/PPO Blended Electrolyte. All of the PVE_x(polyvinylether), $PEPE_x$(Polyepoxide ether) and PAE_x (Polyacrylate ether) materials where x=2-7 were completely amorphous, as indicated by DSC measurements. The T_g is generally below -60°C before addition of Li salts, and increases with increasing salt concentration, particularly when the ratio of ether oxygen to Li ions (O/Li) is less than 15:1. Although the tractable materials exhibited flow and did not form self-standing films, electrochemical measurements could be made by solution casting directly on the electrodes.

An alternative method to form self-standing films is to blend the CB_x materials with high-MW PPO. This material was used to avoid the crystallinity problems that exist with PEO at low temperatures that lead to phase separation. The PPO was Parel Elastomer (Zeon Chemical, MW ~ $5x10^5$) which has a conductivity that is generally two orders lower than that of the CB_x polymers, indicating that the majority of the ion transport in the blends is *via* the CB_x material. However, severe phase separation also occurred which was dependent upon the concentration and identity of the Li salt. This result limits the use of polymer blends in binary salt electrolytes due to concentration polarization.

Lithium-Ion Transference Number (t_+^0) Measurements. The thermal and transport studies on Parel (high-MW PPO)/$Li(CF_3SO_2)_2N$ at 85°C, and amorphous PEO/$LiCF_3SO_3$ and $Li(CF_3SO_2)_2N$ systems at 40°C, were completed. Polarization experiments were carried out to relate the transference number measurements to cycling behavior. As predicted by theory, materials with low or negative transference numbers exhibit rapid polarization at the Li electrode.

Conductivity Limit of Ethylene Oxide-Based Polymers. Conductivity measurements on comb-branch polymers with side chain lengths of 5 ethylene oxide units or longer gave very similar conductivities. The linear amorphous PEO which has ethylene oxide chain lengths of about eight units also had the same conductivity, about 5 x 10^{-5} S/cm at 25°C, regardless of the polymer architecture with $Li(CF_3SO_2)_2N$ as the salt. Intuitively this makes sense as all systems possess the same solvation structures for the Li^+ ions, and the polymer architecture has only a secondary influence. This indicates that new polymers must be prepared that have different structures than ethylene oxide to increase the conductivity to 10^{-3} S/cm at 25°C.

Composite Polymer Electrolytes for Use in Lithium and Lithium-Ion Batteries

Saad A. Khan and Peter S. Fedkiw
Department of Chemical Engineering, North Carolina State University, P.O. Box 7905, Raleigh NC 27695-7905
(919) 515-4519; fax: (919) 515-3465; e-mail: khan@eos.ncsu.edu

Objectives

- Develop solid composite electrolytes utilizing synthesized fumed-silica fillers with tailored surface chemistries.
- Investigate the electrochemical and rheological characteristics of novel composite polymer electrolytes.

Approach

- Utilize a combination of electrochemical and rheological techniques and chemical synthesis to study the effects of silica surface chemistry on the electrochemical and mechanical properties of composite polymer electrolytes.

Accomplishments

- Identified solid electrolytes with high yield stresses, high modulus and room-temperature conductivity of ~10^{-3} S/cm by varying the amount of polymerizable monomer (butyl methacrylate) in the composite system.
- Established experimental techniques and protocols to measure self-diffusion and Li transference number of the composite electrolytes using electrophoretic NMR.
- Developed a scaling relationship to predict *a priori* the solid electrolyte modulus in terms of component properties.

Future Directions

- Determine the transference number in candidate electrolyte systems using the newly developed protocol for electrophoretic NMR.
- Explore interfacial stability of composite electrolytes.
- Develop a comprehensive understanding of the mechanism of crosslinking to produce solid electrolytes with tailored mechanical behavior.

The objective of this research is to develop new composite solid polymer electrolytes for rechargeable Li and Li-ion batteries. In particular, the goal is to develop highly conductive electrolytes that exhibit good mechanical properties, and at the same time show good compatibility with typical electrode materials. The unique feature of our approach is the use of surface-functionalized fumed-silica fillers to control the mechanical properties of the electrolytes. A low-molecular-weight liquid polyether is used as the matrix polymer, thereby ensuring high conductivities, and the fumed silica serves to provide mechanical support.

A key element in the research is to develop protocols to measure transport properties of lithium, anion diffusion and transference numbers using electrophoretic NMR (ENMR).

We have successfully determined the self-diffusion coefficient of Li^+ ions in the composite polymer electrolyte at 30°C. We have recently developed the ability to observe ^{19}F, thus

enabling self-diffusion measurements on the anion. The lithium imide/poly(ethylene glycol) dimethyl ether (PEG-DME)/R805 (octyl-modified) fumed-silica composite electrolyte system is the most studied to date. For the conditions of a Li:O ratio of 1:20, 10 wt% R805 and 30°C, D_{Li} is 3.0±0.2 x 10^{-7} cm^2/sec. This self-diffusion coefficient for of Li^+ ions is comparable to D_{Li} in polymer electrolytes. The fumed silica appears to have only a small effect on the diffusion of Li ions given that for the same system without R805 fumed silica, D_{Li} is about 3.3 x 10^{-7} cm^2/sec. Thus, we conclude that for 10 wt% fumed silica, the mobility of the Li ions is only slightly impeded by the fumed-silica network, a very encouraging result.

The lithium triflate/poly(ethylene glycol) dimethyl ether(PEG-DME)/R805 system with Li:O=1:20, 10 wt% fumed silica, and 30°C was more amenable to ENMR. This is probably due to the much lower anion concentration (fluorine concentration is 3.7 M compared to 6 M). The D_{Li} is 3.2 x 10^{-7} cm^2/sec and D_F is 2.8 x 10^{-7} cm^2/sec, which is comparable to literature values. Preliminary transference numbers for the 5% R805/PEG-DME composite electrolytes containing either lithium imide or lithium triflate salts were higher (0.29) for the imide compared to the triflate (0.19) salt. The calculation and measurement need to be verified, but we are encouraged that we can obtain the behavior expected by ENMR measurements.

Effort was also focused on determining if we can *a priori* predict rheological behavior with electrolytes containing the liquid medium and fumed silica. Octyl-modified fumed silica (R805) in a range of liquids of different polarity was used. We found that the degree of flocculation of the fumed silica to form solids was dictated by the mismatch in solubility parameter between the liquid medium (δ_m) and the surface layer of the fumed silica (δ_s). A scaling relationship between the elastic modulus (G') of the system and the solubility parameters given by G' ~$(\delta_s - \delta_m)^2$ was successfully derived. The practical implication of this result is that it permits us to predict and control one of the important rheological parameter of a composite system.

Studies on the crosslinking mechanism focused on determining the yield behavior of solid polymer electrolytes. While we were successful in obtaining high-modulus solids, the yield stress in these systems were found to be rather low (~1 Pa). A high yield stress (>10^2 Pa) is critical for the electrolyte to perform as a dimensionally stable solid and avoid creep. The yield stress could potentially be enhanced by adding a small amount of polymerizable monomer, such as butyl methacrylate, to the electrolyte that would not detrimentally affect the conductivity (~1x10^{-3} S/cm at 25°C). By varying the amount of butyl methacrylate in a crosslinkable fumed silica/polyethylene glycol dimethyl ether/lithium imide system, we could not only tailor the modulus of the system but also obtain solids with much higher yield stresses (Fig. 15). In Fig. 15, solids with moduli ranging between 4x10^4 and 4x10^5 Pa are obtained by varying the amount of butyl methacrylate. More importantly, the yield stress, defined as the product of G' and strain at onset of sharp decrease (shown by arrow), exceeds 10^3 Pa in both cases. While these results are preliminary, they are very encouraging and work in this direction will continue to understand how composition and crosslinking time affect mechanical properties.

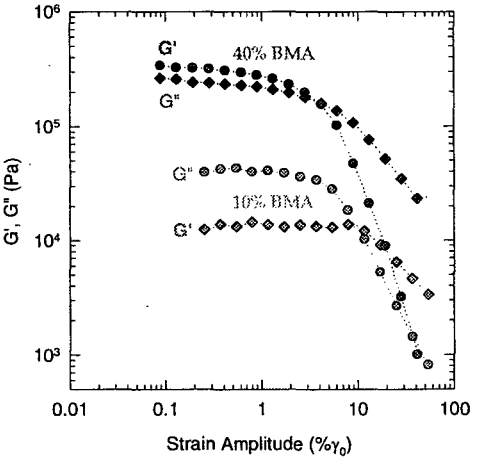

Figure 15. Elastic Modulus (G') as a function of strain amplitude for solid composite electrolytes containing crosslinkable fumed silica fillers. BMA refers to butyl methacrylate contained in the composite.

PUBLICATIONS

J. Fan, S.R. Raghavan, X-Y Yu, J. Hou, G.L. Baker, S.A. Khan, P.S. Fedkiw, "Composite Polymer Electrolytes Using Surface-Modified Fumed Silicas: Conductivity and Rheology," *Solid State Ionics*, **111**, 117-123 (1998).

S.R. Raghavan, M.W. Riley, P.S. Fedkiw, S.A. Khan, "Composite Polymer Electrolytes Based on Polyethylene Glycol and Hydrophobic Fumed Silica: Dynamic Rheology & Microstructure," *Chemistry of Materials* **10(1)**, 244-251 (1998).

S.A. Khan, "Shear-induced Microstructural Changes in Filled Polymers," (invited speaker) *NIST Workshop on Fillers and Nanocomposites*, Gaithersburg, MD, July. 1998.

S.R. Raghavan, J. Hou, G.L. Baker, S.A. Khan, "Colloidal Silica Gels as Novel Electrolytes: Synthesis, Microstructure and Rheology." *ACS National Meeting*, Boston, MA, August 1998.

S.R. Raghavan, J. Hou, G.L. Baker, P.S. Fedkiw, S.A. Khan, "A Novel Polymer Electrolyte Incorporating Crosslinkable Particles into a Composite Polymeric Framework," AIChE Annual Meeting, Miami, FL, November 1998.

Polymer Electrolyte for Ambient-Temperature Traction Batteries: Molecular-Level Modeling for Conductivity Optimization

Mark A. Ratner
Department of Chemistry, Northwestern University, Evanston IL 60208-3133
(847) 491-5371, fax: (847) 491-7713; e-mail: ratner@mercury.chem.nwu.edu

Objectives

- Explore conductivity mechanisms in polymer/salt complex Li-based soft electrolytes to identify the role of salt, anion, dynamics of the polymer host solvent, and coupling between relaxation and transport on conductivity.
- Develop a predictive capability based on electronic structure calculations and formal site models to optimize polyelectrolyte-based soft electrolytes for Li batteries.
- Identify optimized composite structures that utilize inorganic fillers in the polymeric hosts to obtain high cation transference number and ion mobility.

Approach

- Use theoretical models, both of electronic structure type and of dynamical transport type, to understand and predict the effects of specific variation of variables (temperature, density, salt choice, filler size, plasticizer, thermal history) on conductivity of polymer-based electrolytes.

Accomplishments

- Predicted and analyzed anionic electron density that produce higher numbers of mobile ions in polyelectrolytes, and identified optimized aluminosilicate structures for simple polyelectrolytes and composites
- Completed *ab-initio* calculations on polyelectrolyte structures, identifying mechanistically the ion-dipole interactions that control free carrier number, and how to optimize them by polymer design.

- Completed a formal, doubly harmonic analytical model for analyzing and predicting effects of polymer stiffness, site density, temperature and ionic radius on ion mobilities.

Future Directions

- Develop new methods to identify nanocomposite structures and hard polymer/salt complexes.
- Investigate the nature of the softening mechanism (how does the nanocomposite inorganic filler lower the glass transition behavior of the polymeric host), and to optimize the free carrier density based on this same local electronic structure in polyelectrolytes.

The effort is based on the idea that appropriate theoretical models, closely coupled with experimental advances and measurements, can identify improved polymer electrolytes for Li batteries. Polymer electrolytes were discovered about 25 years ago, but most of the ideas (coupling of relaxation to transport, low-glass-transition hosts, charge delocalized counter-ions) have not been meaningfully extended in the last decade. The aim of this research is to focus more explicitly on experimental modifications to optimize the conductivity properties (and the compliance properties and stability properties) of polymer electrolytes.

The polymer/salt neat complexes were extensively investigated, but they suffer from low conductivity (at best, ambient-temperature conductivities near 10^{-4} S/cm are reported), and cation transference numbers are < 0.5, leading to anion motion, cell polarization and inefficient current flow. One solution to the problems is to develop a stiff electrolyte with sufficient available free volume that decoupling can be attained. Theoretical analysis of these structures has suggested both that decoupling occurs, and that the conductivity should be of simple Arrhenius rather than bent WLF type. This is observed, and ambient-temperature conductivities are equal to those of the best previous polymer/salt complexes.

Polyelectrolytes of polymer-based structures in which the anionic charge is bonded to the polymer backbone was investigated. These materials have unit transference number for Li^+ ions, therefore minimizing cell polarization. The difficulty to date has been that their conductivities are even lower (often by a factor of 100) than the polymer/salt complexes. Two research efforts aimed at improving the polyelectrolyte conductivity were completed. Using *ab-initio* calculations (in collaboration with Larry Curtiss at Argonne National Laboratory), we have shown that aluminosilicates, which provide lower local-bond dipole densities, show weaker Lewis basicities than aluminates, silicates, or borosilicates. This suggests that aluminosilicate structures will be ideal polyelectrolyte hosts, both in simple structures and in composites. This is one of the first uses of *ab-initio* methodology in polymer electrolytes, and it provides an important conceptual link between design of materials and transport properties.

A simple, doubly harmonic analytical model for understanding how host softness and ion size, as well as carrier density, affect ionic conductivity in Li polyelectrolytes was completed. While this model is simple, it provides analytic (as opposed to simply numerical) predictions, and therefore can be used to design host polyelectrolyte structures with optimized conductivity properties.

Polymer-based electrolytes that comprise composites, particularly organic hosts with inorganic fillers were analyzed. Two aspects were studied: (i) *ab-initio* calculations suggest that the silicate structures are not ideal, because there are insufficient free ions; (ii) the substantial variations in the glass transition temperature in nanocomposite materials, as opposed to macrocomposite materials, strongly suggests that one can optimize the coupled transport (as opposed to the decoupling transport discussed above), and therefore this nanocomposite polyelectrolyte structure would have unit transference number, high mobility,

high conductivity and stable compliance properties.

While the modeling in this area has just begun, it will constitute the major effort in the future.

PUBLICATIONS

E. Sim, A.Z. Patashinski and M.A. Ratner, "Glass Formation and Local Disorder: Amorphization in Planar Clusters," *J. Chem. Phys.* **109**, 7901-7906 (1998).

M. Ratner, "Mathematics, Computational Chemistry, and Battery Building: Some Notions, in Modeling and Computation for Applications in Mathematics, Science, and Engineering," J.W. Jerome, ed., Oxford University Press, 1-24 (1998).

J. Kolafa and M. Ratner, "Oligomers of Poly(Ethylene Oxide): Molecular Dynamics with a Polarizable Force Field," *Molecular Simulation* **21**, 1-26 (1998).

Corrosion of Current Collectors in Rechargeable Lithium Batteries

James W. Evans (Lawrence Berkeley National Laboratory)
585 Evans Hall, MC 1760, University of California, Berkeley CA 94720
(510) 642-3807, fax: (510) 642-9164; e-mail: evans@socrates.berkeley.edu

Objectives

- Examine corrosion of current collectors in Li-polymer and Li-ion batteries.
- Develop corrosion-resistant collectors and/or corrosion inhibition approaches.
- Develop the electrochemical quartz crystal microbalance as a tool for investigating reactions in Li batteries.

Approach

- Use electrochemical and electrochemical quartz crystal microbalance (EQCM) techniques to develop understanding of the corrosion behaviour of current collectors and corrosivity of various electrolytes, along with other reactions limiting the performance/lifetime of Li cells.
- Measure rates and identify corrosion processes of current collectors in Li batteries under different charge conditions and systems by SEM analyses.

Accomplishments

- Identified the most serious pitting corrosion of Al current collectors in Li-polymer batteries among the combination of four salt candidates ($LiClO_4$, $LiCF_3SO_3$, Li imide and Li methide) and four cathode candidates ($LiMn_2O_4$, $LiCoO_2$, TiS_2 and V_6O_{13}) during overcharging in the system Li / PEO + $LiCF_3SO_3$ / TiS_2 ..
- Observed from EQCM data that solvent oxidation and salt oxidation are more severe than corrosion of Al (when the Al is protected by a passivating film) at high oxidation potentials in contact with PC + Li imide.

Future Directions

- Identify corrosion products on the surface of Al current collectors using the EQCM technique.
- Develop a new solvent stable up to high oxidation potential such as ethylmethylsulfone and evaluate its performance.

Potentiodynamic scans were used to investigate the corrosion behavior of current collectors in the presence of Li salt ($LiClO_4$, $LiCF_3SO_3$, Li imide and Li methide) in conventional electrochemical cells (consisting of Al working electrode, a counter electrode and a reference electrode with a Li salt/PEO electrolyte). Pitting corrosion was previously identified as the most severe form of corrosion experienced by Al in these cells. Only a few pits were observed on the Al working electrode after cyclic potentiodynamic anodic polarization up to 5 V (*vs.* Li/Li^+) with three Li salts ($LiClO_4$, Li imide and Li methide). However $LiCF_3SO_3$ showed an increase in current density with cycle number and the collector displayed severe pitting corrosion. The current density in this system increases to over $0.1 mA/cm^2$, which is equivalent to a penetration rate of 1 mm/year, in the potential region 4.2 V. Therefore, $LiCF_3SO_3$ cannot be used when the operating voltage above 4.2 V are encountered due to the corrosion of Al current collectors.

To investigate the corrosion behavior of the current collectors for the composite cathode ($LiMn_2O_4$, $LiCoO_2$, TiS_2 and V_6O_{13}), cells consisting of a positive electrode, a negative electrode, and the appropriate current collectors were employed. From the selection of $LiMn_2O_4$, $LiCoO_2$, TiS_2 and V_6O_{13}, pitting corrosion of Al current collectors is the most severe with TiS_2. Direct SEM showed that pitting corrosion of Al initiates below 4 V. Efforts to elucidate the cause of corrosion of Al current collectors attached to composite cathodes were made by varying the amount of cathode material or carbon. However the composition change had little effect on Al corrosion.

Corrosion measurements with the EQCM were conducted in carbonate-based propylene carbonate (PC) or ether-based poly(ethylene glycol) dimethyl ether (PEGDME) solutions containing $LiPF_6$ or Li imide. The EQCM enables us to observe very small mass change of an electrode such as Al by measuring the frequency change of a quartz crystal on which the Al is placed as a film. From the mass change, the species that take part in corrosion and passivation is revealed. There was no evidence of severe corrosion of as-received Al, which is protected by Al_2O_3 produced by atmospheric oxidation, in either $LiPF_6$ or Li imide. Even though the oxidation current was high, the mass change of Al was very small, indicating that solvent oxidation and salt oxidation is more severe than Al corrosion at the high oxidation potentials used. However, the situation is different for Al polished in the Ar atmosphere in a glove box. It appears that Al reacts with the anion of Li imide and forms soluble corrosion products. On the other hand, Al is likely to form insoluble corrosion products in $LiPF_6$ system. These investigations suggest that damage of the Al during manufacture of batteries in protective atmospheres may lead to pitting corrosion.

Development of Novel Chloroaluminate Electrolytes for High-Energy-Density Rechargeable Lithium Batteries

Kraig A. Wheeler
Department of Chemistry, Delaware State University, Dover DE 19901
(302) 739-4934, fax: (302) 739-3979; e-mail: kwheeler@dsc.edu

Objectives

- Develop electrochemically stable sulfone electrolytes.
- Characterize and investigate the electrochemical and physical properties of these electrolytic materials for lithium rechargeable battery (LRB) applications.

Approach

- Synthesize sulfones by direct alkylation of mercaptan, followed by further oxidation
- Evaluate electrochemical and spectroscopic properties of electrolytes.

Accomplishment

- Reproducibly synthesized three aryl sulfones using nonaqueous, inert atmosphere techniques.

Future Directions

- Develop and characterize organic-based electrolytes with improved electrochemical stability for LRB.
- Investigate the electrochemical properties of sulfones in collaboration with Case Western Reserve University.

The program focuses on the synthesis and demonstration sulfone electrolytes with improved electrochemical stability in rechargeable Li batteries. Sulfone-based electrolytes represent materials with improved stability towards electrochemical processes as well as reduced chemical toxicity. This program is directed towards the design and synthesis of stabilized sulfone electrolytes.

The major thrust of the program is to synthesize a family of structurally related sulfone-based compounds (**1** - **4**). These solvents were systematically chosen to investigate the effect of varying the electron-donating/withdrawing ability of R and R'. Because of the electron-donating ability of the phenyl group, phenyl sulfones possess a stronger C-S bond resulting in greater stability towards oxidation/reduction.

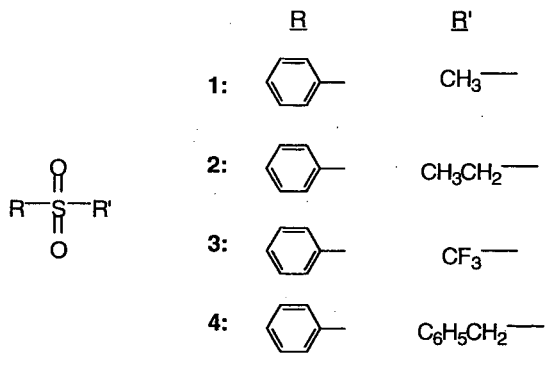

Aryl sulfones **1**, **2**, and **4** have been successfully synthesized in reasonable quantities (Fig. 16) by direct alkylation of the phenyl mercaptan, which formed the sulfide, followed by further oxidation with meta-chloroperbenzoic acid (MCPBA). These materials have been fully characterized by ^{1}H-NMR spectroscopy. The successful syntheses and characterization of aryl sulfones **1** – **4** nearly completes phase one of this project.

The second phase of this project centers on the purification and electrochemical studies of aryl sulfones **1** – **4**. Through a grant from DOD, we have recently been able to obtain an inert atmosphere glove box and a bipotentiostat to conduct electrochemical studies of the electrolyte. The acquisition of this equipment will permit us to freely study and manipulate these aryl sulfone compounds.

The glove box (Vacuum Atmospheres) was installed in January 1999 and the purification of samples **1**, **2**, and **4** in an inert atmosphere followed. The project's capacity and strength at DSC centers on organic methodologies and characterization. As a result, in order to also become proficient in electrochemical studies select personnel at DSU will travel to CWRU in April 1999 to be trained on the operation and application of the newly purchased bipotentiostat equipment. Such a collaboration will not only provide the essential skills to investigate the electrochemical properties of sulfones **1** – **4**, but also strengthen the overall program at DSU in the area of electrochemical methods and applications.

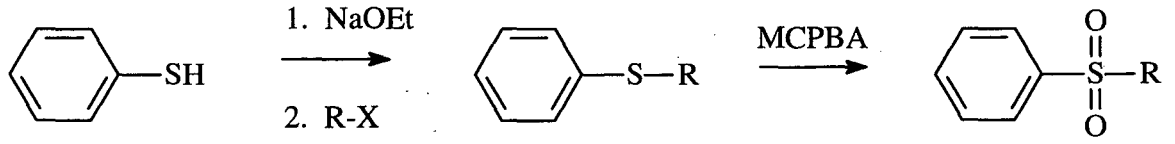

Figure 16. Synthetic scheme for the preparation of aryl sulfones **1 – 4**.

CROSS-CUTTING RESEARCH

Cross-cutting research is carried out to address fundamental problems in electrochemistry, current-density distribution and phenomenological processes, solution of which will lead to improved electrode structures and performance in batteries and fuel cells.

Analysis and Simulation of Electrochemical Systems

John Newman (Lawrence Berkeley National Laboratory)
201 Gilman Hall, MC 1462, University of California, Berkeley CA 94720
(510) 642-4063, fax: (510) 642-4778; e-mail: newman@newman.cchem.berkeley.edu

Objectives

- Improve the performance of rechargeable electrochemical cells by identifying the controlling phenomena.
- Identify important parameters which are crucial in the operation of an advanced secondary battery.
- Determine transport and other properties for electrochemical applications.

Approach

- Develop and implement mathematical models, computer programs, and characterization experiments to describe phenomenologically Li batteries and components.

Accomplishments

- Developed and demonstrated a Monte Carlo computer program to describe the concentration dependence of the diffusion coefficient in a Li-intercalation electrode.
- Simulated a hybrid electric vehicle using a detailed battery model to guide design and operation.

Future Directions

- Assess quantitatively a transport model for a plasticized, polymer electrolyte.
- Continue development of molecular dynamics program to determine diffusion coefficients in electrolyte systems.
- Develop improved experimental and theoretical model for thermal management of Li batteries.

This program rigorously researches fundamental electrochemical phenomena and the impact on rechargeable batteries for electric and hybrid vehicles. Mathematical models with minimal assumptions are developed to create computer programs and guide experimental efforts. In-house numerical codes solve derived systems of equations to study coupled transport, kinetic, and thermodynamic problems of electrochemical interest. Experimental studies seek to provide information crucial for model implementation. The overall effort results in design and operational guidelines for electrochemical devices and components.

Cathode studies. The dependence of the diffusion coefficient of Li^+ ions in the $Li_yMn_2O_4$ lattice on concentration was modeled. A statistical, Monte Carlo approach was implemented to model the short-time diffusion of Li. This simulation method determines the variation of diffusion coefficient with concentration.

A 3-dimensional lattice model captures the variation of the diffusion coefficient. The model system consists of a region of fixed temperature, volume, and Li intercalant occupancy in the host lattice. Using a discretized grid, a block (high concentration) of particles is permitted to move instantaneously into the surrounding, void (low concentration) space. Monitoring the movement of Li atoms over simulation time enables the calculation of overall and "jump" diffusion coefficients. The latter is the component limited purely by occupancy (concentration). A thermodynamic component is tractable from repeated computations. Canonical ensembles are equilibrated over a range of occupancy and temperature.

The results qualitatively match the measured diffusion coefficients over a range of concentrations. Only trends are calculable by the implemented Monte Carlo technique. Absolute values cannot be determined, giving rise to one fitting (scaling) parameter. Simulation results agree particularly well with experiments at low Li state of charge.

Hybrid vehicles. Another modeling effort involved the load leveling of hybrid vehicles using dual Li intercalation electrodes. The hybrid configuration consisted of a drive train that derived steady power from a conventional engine, with a Li battery for instantaneous power requirements. Parameters adjusted for optimal performance included salt concentration, electrode porosity, electrode thickness, and porous phase particle sizes. Batteries were optimized over a six-minute, partially urban driving cycle.

One study compared optimization by fuel economy *vs.* minimal battery size. The system results with minimum fuel consumption were compared with output for minimum electrode area. The area-minimized case yielded a fuel economy close to the maximum. In other words, no significant advantage in gas mileage was gained in optimizing with respect to fuel economy *vs.* size.

An analysis of the benefit of regenerative braking was also completed. Batteries were optimized over the previously mentioned driving cycle with three different percentages of brake energy recovery. A promising result was that the zero-emission range (or distance accessible without conventional power) was nearly 40 miles with 66% recovery. Maximum battery power, zero-emission vehicle range, and energy efficiency increased with available brake recovery. Unfortunately, size and weight increased with percent recovery as well.

Additional simulations have addressed the tradeoff between fuel economy and power. Previous optimizations of fuel economy subjected a hybrid-vehicle model to a six-minute driving cycle. A subsequent investigation utilized a more stringent one-minute cycle with greater power requirements. Optimized by the same criterion as for the six-minute cycle, the system demonstrated 10% fewer miles per gallon of gasoline consumed. This result was due to the 150% increase in battery weight and lower cycle efficiency. A positive finding, however, was the three-fold increase in zero-emission vehicle range. This measure of the total capacity is the distance travelable under battery power alone.

An additional investigation considered fuel economy for various vehicle weights, using the six-minute driving cycle. Heavier vehicles require larger, less-efficient batteries to satisfy

the power requirements of the cycle, and the mileage-per-gallon decreased roughly linearly with an increase in vehicle weight.

Transport studies. An effort has continued to determine the transport properties in polymer electrolytes. Initial work entailed the development of a mathematical model to derive the desired properties from experiments. A model for transport was derived to calculate the diffusion coefficient(s), transference number and conductivity. The molar fluxes were expressed linearly in terms of the driving forces. These forces were the gradients of potential, solvent concentration, and salt concentration. Experimental steady-state flux or transient concentration profiles would then enable the calculation of properties through the linear relations. An understanding of the governing transport equations proved important in deciding the necessary techniques and measurements.

For the acquisition of new data on plasticized polymer electrolytes and other electrochemical systems, a new laboratory facility was established. This laboratory houses an argon-atmosphere glovebox for work involving oxygen-sensitive or water-sensitive chemistries. Its electrochemical analysis capabilities include impedance spectroscopy, heat conduction calorimetry, and cyclic voltammetry. Currently, the verification of the galvanostatic polarization method, a crucial experimental technique, is sought. This technique is chosen to measure the cation transference number. Modification of the necessary instrumentation is underway. A model cell (silver, potassium chloride, and silver chloride) with known properties is constructed for diagnostic testing.

Another effort involves a molecular dynamic simulation to obtain transport properties of liquid electrolytes. For such nonideal systems, a computer program is being developed to determine the concentration dependence of the diffusion coefficient. Molecular dynamics relies upon the knowledge of the potential function between atoms, molecules, or ions. A promising, novel approximation using the Fourier transform is being implemented to capture long-range electrostatic forces in electrolyte systems.

Thermal management. New work has begun in the thermal management of electrochemical cells. To address heat generation and thermal stability issues of intercalation systems, a small model cell has been constructed. This centimeter-scale coin cell includes a Li foil anode, a polymer electrolyte separator, and a spinel cathode. Common solvent and electrolyte are used for comparison with a commercial system. The cathode is a mixture of lithium manganese oxide intercalant and carbon. Initial diagnostic testing of the system is underway.

Double-layer capacitors. The steady operation of porous carbon double-layer capacitors was evaluated. First, a resistance model was developed considering macroporosity, a large particle-to-solution conductivity ratio, and kinetic overpotential. The performance over a range of porosities and thicknesses were considered. The results from various discharge profiles were compiled into dimensionless, universal curves that can be used in deciding the design properties and cycle times for a given application. Specific power and percent recovery of available energy were calculated for galvanostatic and constant-power discharges. This model quantitatively confirmed the reported potential applications of double-layer capacitors for frequent-cycle, short-discharge energy storage. On the other hand, batteries and other storage devices prove more effective in power delivery over minute or longer time scales. The concentration overpotential and microposity were evaluated. Gradients and, thus, overpotential are small for electrolyte concentrations on the order of 1 M or greater. However, pores below a critical dimension may be too small to allow ions to enter. In this case, the system cannot deliver the calculated energy density because of inaccessible electrode area.

PUBLICATIONS

M.L. Perry, E.J. Cairns and J. Newman, "Mass Transport in Gas-Diffusion Electrodes: A Diagnostic Tool for Fuel-Cell Cathodes," *J. Electrochem. Soc.* **145**, 5 (1998).

R. Darling and J. Newman, "Modeling Side Reactions in Composite $Li_yMn_2O_4$ Electrodes," *J. Electrochem. Soc.* **145**, 990 (1998).

T. Jones, J. Newman, and other Standing Committee members, Review of the Research Program of the Partnership for a New Generation of Vehicles, Board on Energy and Environmental Systems, Commission on Engineering and Technical Systems, Transportation Research Board, National Research Council, Washington, D.C.: National Academy Press, 1998.

K.P. Ta and J. Newman, "Mass Transfer and Kinetic Phenomena at the Nickel Hydroxide Electrode," *J. Electrochem. Soc.* **145**, 3860 (1998). LBNL-41467.

R.M. Darling, "Lithium Manganese Oxide Spinel Electrodes," *Ph.D. Dissertation*, December 1998.

Electrode Surface Layers

Frank R. McLarnon
90-1142 , Lawrence Berkeley National Laboratory, Berkeley CA 94720
(510) 486-4636, fax: (510) 486-4260; e-mail: frmclarnon@lbl.gov

Objectives

- Apply advanced *in situ* and *ex situ* characterization techniques to study the structure, composition, formation and growth of surface layers on electrodes used in rechargeable batteries.
- Identify film properties that improve the rechargeability, cycle-life performance, specific power, specific energy, stability and energy efficiency of electrochemical cells.

Approach

- Use ellipsometry, Raman spectroscopy, scanning probe microscopy, impedance analysis and other methods to characterize surface layers on secondary battery electrodes.
- Determine changes in electrode structure and surface morphology which accompany charge-discharge cycling, and seek new electrode-electrolyte combinations which lead to enhanced cell cycle-life performance.

Accomplishments

- Completed spectroscopic and microscopic studies of Ni electrodes in alkaline electrolyte, and elucidated the roles of Co and Li additions.
- Discovered a novel photochromic-electrochromic material based on $Ni(OH)_2$ and TiO_2.

Future Directions

- Use optical, spectroscopic and microscopic techniques to characterize surface layers on Li, carbon and metal oxide electrodes in non-aqueous electrolytes.

The primary objective of this research is to identify film properties that improve the rechargeability, cycle-life performance, specific power, specific energy, stability, safety and energy efficiency of electrochemical cells. Advanced *in situ* and *ex situ* techniques are employed to characterize surface layers (solid

electrolyte interfaces, SEIs) on electrodes used in rechargeable batteries.

The behavior of Ni electrodes in alkaline electrolyte was investigated to better understand the cause(s) of limited initial capacity, capacity fade and poor coulombic efficiency of this important electrode. Research on the electrochemical behavior of thin electroprecipitated $Ni(OH)_2$ films, a geometry which models the regions of active material in a practical battery electrode was completed. Raman spectroscopic studies were complemented by using *in situ* atomic force microscopy (AFM) to investigate the effects of charge-discharge cycling, Co co-precipitation and the uptake of Li from the electrolyte on the film morphology. A Ni substrate was selected, in contrast to studies described in the literature which use a highly oriented pyrolytic graphite substrate, because we believe that interactions between the electrochemically active $Ni(OH)_2$ film and the substrate play a key role in electrode performance of a practical battery electrode.

An AFM image of a freshly deposited pure $Ni(OH)_2$ film obtained at open-circuit potential (0.13 V *vs.* Hg/HgO) showed ~700-nm aggregates with clearly defined boundaries. A single charge-discharge cycle transformed the film morphology into a structure of closely packed 50-nm grains. Further cycling led to the formation of deep crevices and produced a highly disordered film with non-uniform electrochemical activity. The areas close to mechanical fissures accumulated material, most likely products of Ni substrate oxidation. AFM images of the film in its reduced and oxidized states after 60 cycles revealed that the film morphology varied strongly with the state-o-charge of the electrode (Fig. 17). *In situ* monitoring of a specific location on the film surface at different potentials showed that the expansion and contraction that accompany charging and discharging are non-uniform and site selective. This finding supports our Raman spectroscopy results which revealed the formation of a new inactive phase as the electrode was cycled and linked this phase with electrode capacity loss.

An AFM image of a freshly precipitated $Ni(OH)_2$ film with 11 wt% Co showed that Co induces significant modifications in the film microstructure, *i.e.*, a compact structure of elongated randomly oriented ~200-nm grains was formed when Co is incorporated into Ni sites. A single charge-discharge cycle induced significant changes in the film microstructure, transforming it into a globular structure with ~150-nm grains, similar to that of a pure $Ni(OH)_2$ film. This type of film structure was present in both the reduced and oxidized states, and remained almost unchanged after 60 cycles. These results agree with our correlation between voltammetric peaks and Raman spectra, and taken together our results provide a rather convincing explanation of the role Co plays in stabilizing the Ni electrode capacity.

In situ AFM measurements of electroprecipitated $Ni(OH)_2$ films in 0.9 M NaOH + 0.1 M LiOH electrolyte revealed that Li^+ ions have a significant effect on the film morphology. AFM images of pure $Ni(OH)_2$ showed a cluster structure with grain sizes ranging from 50 to 150 nm, however in the presence of Li^+ ions the film morphology remained almost unchanged during early cycles. Prolonged cycling produced a rough and highly non-uniform surface topography, although very little change occurred during charging and discharging. AFM measurements of Co-doped $Ni(OH)_2$ films in the Li^+-containing electrolyte fully supported our electrochemical and spectroscopic data. AFM images revealed a very uniform compact granular structure was formed which remained stable during potential excursions and cycling.

The effect of Ni-film interfacial processes on electrode performance was investigated to detect the products of these processes, determine their formation mechanisms and assess their roles in electrode. The goal is to develop Ni substrate processing steps to improve electrode performance. In an attempt to identify corrosion reactions, a series of chronoamperometric measurements was carried out. A freshly electroprecipitated thin-film $Ni/Ni(OH)_2$ electrode was polarized at 0.0 V in 1 M NaOH, *i.e.*, a potential at which the $Ni(OH)_2$ phase remains in thermodynamic equilibrium

with pure Ni. Surprisingly, electrode polarization was always accompanied by significant anodic currents that decayed exponentially in time. This current could not be attributed to charging of the active material because the electrode potential was ~450 mV below that for $Ni^{(II)} \rightarrow Ni^{(III)}$ oxidation. A possible contribution might arise from the oxidation of H_2 trapped in the $Ni(OH)_2$ film during the cathodic precipitation process, however similar measurements conducted with a Pt substrate showed anodic currents one order of magnitude smaller than at Ni. These results led us to conclude that the $Ni^{(0)}_{(substrate)} \rightarrow Ni^{(II)}_{(interfacial\ film)}$ oxidation reaction proceeds at the Ni substrate in spite of the presence of the $Ni(OH)_2$ film. The product of anodic Ni substrate corrosion can not only add capacity to the electrode, it can also explain the frequent observation of excess anodic capacity during the first cycle. On the other hand, too much corrosion can weaken the Ni substrate and lead to poor contact with the active material. There is also the possibility that the Ni corrosion products may have composition and electrochemical properties that differ from those of electroprecipitated $Ni(OH)_2$.

To gain deeper insight into this problem another series of tests was conducted. Prior to $Ni(OH)_2$ precipitation, the Ni substrate was repetitively cycled in 1 M NaOH between 0.0 and 0.6 V at 10 mV/s for 2 h. Although this cycling led to the formation of an electrochemically active passive layer (documented by a pair of $Ni^{(II)} \leftrightarrow Ni^{(III)}$ voltammetric peaks), a $Ni(OH)_2$ film subsequently electroprecipitated on top of it performed very poorly, and the electrode capacity decayed much faster than usual.

PUBLICATIONS AND PRESENTATIONS

F. Kong, R. Kostecki, F. McLarnon and R.H. Muller, "Spectroscopic Ellipsometry of Electrochemical Precipitation and Oxidation of Nickel Hydroxide Films," *Thin Solid Films*, **313-314**, 775-80 (1998).

F. Kong, R. Kostecki and F. McLarnon, "*In Situ* Ellipsometric Study of the Electroprecipitation of Nickel Hydroxide Films," *J. Electrochem. Soc.* **145**, 1174-78 (1998).

R. Kostecki, T. Richardson and F. McLarnon, "Photochemical and Photoelectrochemical Behavior of a Novel $TiO_2/Ni(OH)_2$ Electrode," *J. Electrochem. Soc.*, **145**, 2380-85 (1998).

F. Kong, J. Kim, X. Song, M. Inaba, K. Kinoshita and F. McLarnon, "Exploratory Studies of the Carbon/Nonaqueous-Electrolyte Interface by Electrochemical and *In Situ* Ellipsometry Measurements," *Electrochemical and Solid State Letters*, **1**, 39-41 (1998).

J. Kim, F. Kong, X.Y. Song, M. Inaba, K. Kinoshita and F. McLarnon, "Studies of the Carbon/Nonaqueous Electrolyte Interface by Electrochemistry, *In Situ* Ellipsometry and Impedance Spectroscopy," paper no. 72 presented by J. Kim at the *193rd Meeting of the Electrochemical Society*, San Diego, CA May 1998.

R. Kostecki and F. R. McLarnon, "*In Situ* Atomic Force Microscopy Study of Co and Li-Doped Nickel Hydroxide Films," paper no. 36 presented by R. Kostecki at the *194th Meeting of the Electrochemical Society*, Boston, MA November 1998.

M. Inaba, R. Kostecki, K. Kinoshita and F. McLarnon, "Ti-, Zr-, Nb- and Mo-Doped Lithium Manganese Oxide Positive Electrodes," paper no. 125 presented by M. Inaba at the *194th Meeting of the Electrochemical Society*, Boston, MA November 1998.

R. Kostecki and F. McLarnon, "Novel Monolithic Electrochromic Device Controlled by Incident Illumination," LBNL Provisional Patent Application (1998).

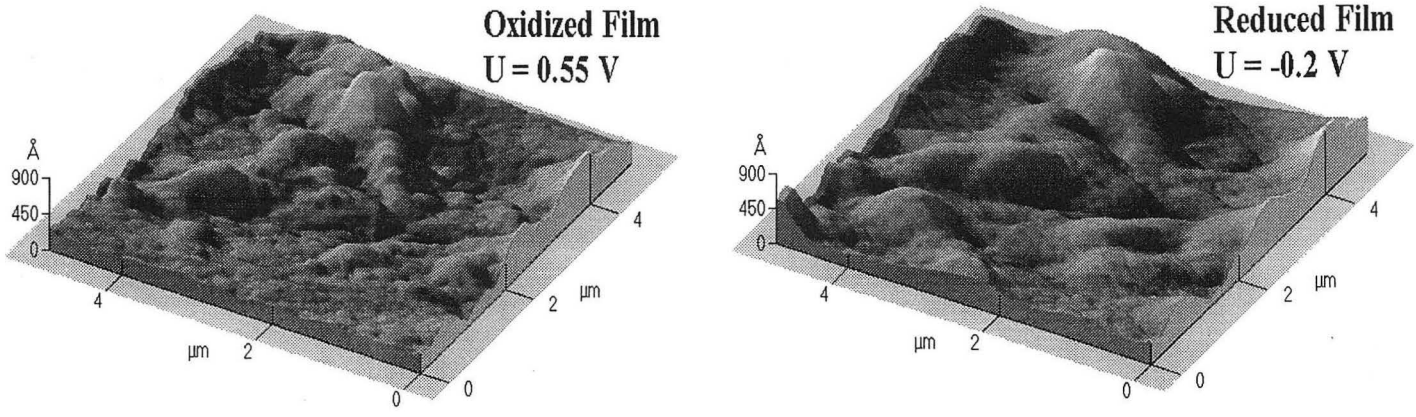

Figure 17. AFM images of a $Ni(OH)_2$ film after 60 cycles in 1.0 M NaOH

Lithium Electrode Interfacial Studies

Philip N. Ross, Jr.
2-100, Lawrence Berkeley National Laboratory, Berkeley CA 94720
(510) 486-6226, fax: (510) 486-5530; e-mail: pnross@lbl.gov

Objectives

- Develop an understanding at the molecular level of the reactions that occur at the Li/electrolyte interface to form the solid electrolyte interfacial (SEI) layer.
- Investigate the role of solute ions and solvent impurities (such as water) on the film forming process.

Approach

- Apply a combination of UHV surface analytical methods and *in situ* ellipsometry.

Accomplishments

- Studies of the reactions of clean metallic Li with the following solvents were completed: ethers - 1,3 dioxolane and 1,2 dimethoxyethane (DME); carbonates - dimethyl carbonate (DMC) and diethylcarbonate (DEC).
- A study of the reaction of clean metallic Li with CO_2 was completed.

Future Directions

- Study the interaction of LiC_6 with the solvents used in Li-ion batteries, *e.g.*, DMC and DEC.
- Study the chemistry of intercollation of Li in graphite in UHV using photoelectron spectroscopy.

The reactions of dimethyl carbonate (DMC) and diethyl carbonate (DEC) with clean metallic Li in UHV were studied by X-ray photoelectron spectroscopy (XPS) using a temperature-programmed-reaction methodology. Both molecules are of interest as solvents in ambient-temperature Li batteries. The solvent molecules were condensed onto the surface of an evaporated Li film at 120 K, and spectra were collected as the sample was warmed in ca. 25 - 30 K increments. The reaction of either DMC or DEC with Li was initiated at 180 K, a temperature much lower than their bulk melting temperatures, producing lithium methyl carbonate, methyl lithium and lithium ethyl carbonate and ethyl lithium, respectively. At temperatures above 270-300 K, the lithium alkyl carbonates start to decompose with Li_2O, elemental carbon and alkyl lithium as products on the surface. Both DMC and DEC are more reactive towards metallic Li than propylene carbonate. Since methyl and ethyl lithium are highly soluble in the parent solvent, electrodeposited Li is predicted to have poor stability in an electrolyte composed of either DMC or DEC:

A study of the reactions of clean metallic Li with two other prototypical ethereal solvents, 1,2 dimethoxyethane (DME) and 1,3 dioxolane (1,3-DOL) was also completed using the same methodology. The interfacial reactions were distinctly different for the two solvents. The reaction of Li with DME has similarities to the reaction with tetrahydrofuran (THF) studied previously. Initiation of the reaction occurs upon melting of the condensate layer at ca. 220°K, with cleavage of the RCH_2-OCH_3 bond and formation of CH_3O-Li and $CH_3OCH_2CH_2$-Li, and a small amount of ethylene. Unlike THF, however, there is no evidence of polymerization. In contrast, polymerization of 1,3-DOL is the *only reaction* occurring at the interface throughout the temperature range of 180–300°K. The polymer consists of a mixture of the repeat units $-CH_2CH_2$ CH_2-, $-OCH_2O$-, and $-OCH_2CH_2$- in the ratio of approximately 1:1:2. The mechanism of this polymerization is unknown to us, but our spectroscopic data clearly indicate it is probably initiated without the formation of an RO-Li intermediate. Thus, 1,3 DOL is the least reactive solvent of any that we have studied, and forms a SEI layer that is close to the same molecular conformation as the solvent itself. This surface chemistry explains the high cycling efficiencies of Li in electrolytes based on 1,3 DOL.

PUBLICATIONS

G. Zhuang, K. Wang, Y. Chen, and P. Ross, "Study of the Reactions of Li with Tetrahydrofuran and Propylene Carbonate by Photoemission Spectroscopy," *J. Vac. Sci. and Technol. A*, **16**, 3041 (1998).

G. Zhuang, Y. Chen, and P. Ross, "The Reaction of Li with Carbon Dioxide Studied by Photoelectron Spectroscopy," *Surf. Sci.*, **418**, 139 (1998).

G. Zhuang, Y. Chen, and P. Ross, "The Reaction of Li with Dimethyl Carbonate and Diethyl Carbonate in UHV Studied by XPS," *Langmuir*, **15**, 470 (1999).

ACKNOWLEDGMENTS

This work was supported by the Assistant Secretary for Energy Efficiency and Renewable Energy, Office of Advanced Automotive Technologies of the U.S. Department of Energy under Contract No. DE-AC03-76SF00098. The support from DOE and the contributions by the participants in the ETR Program are acknowledged. The assistance of Ms. Susan Lauer for coordinating the publication of this report and Mr. Garth Burns for providing the financial data are gratefully acknowledged.

LIST OF ACRONYMS

AFM	atomic force microscopy
BET	Brunauer-Emmett-Teller
BNL	Brookhaven National Laboratory
CB	comb-branch
DEC	diethyl carbonate
DMC	dimethylcarbonate
DME	dimethoxyethane
DOD	Department of Defense
DOE	Department of Energy
DOL	dioxolane
DSC	differential scanning calorimetry
DTA	differential thermal analysis
ECPS	electrochemical potential spectroscopy
EC	ethylene carbonate
EIS	electrochemical impedance spectroscopy
EMA	effective medium approximation
EMC	ethyl methyl carbonate
ENMR	electrophoretic nuclear magnetic resonance
EQCM	electrochemical quartz crystal microbalance
ETR	Exploratory Technology Research
EV	electric vehicle
EXAFS	extended X-ray absorption fine structure
HDPE	high density polyethylene

HQ	HydroQuebec
ICL	irreversible capacity loss
LBNL	Lawrence Berkeley National Laboratory
LLNL	Lawrence Livermore National Laboratory
LRB	lithium rechargeable battery
MCMB	mesocarbon microbead
MCPBA	meta-chloroperbenzoic acid
MW	molecular weight
NMR	nuclear magnetic resonance
PAE	polyacrylate ether
PC	propylene carbonate
PDI	polydispersity indices
PEG-DME	polyethylene glycol - dimethyl ether
PEMO	polyethylene-methylene oxide
PEO	poly(ethylene oxide)
PEPE	polyepoxide ether
PNGV	Partnership for a New Generation of Vehicles
PPO	polypropylene oxide
PVE	polyvinylether
SEI	solid electrolyte interface
SEM	scanning electron microscopy
SOC	state-of-charge
TCO	tin-based composite oxide
TEM	transmission electron microscopy
TGA	thermogravimetric analysis
THF	tetrahydrofuran
TMA	tetramethyl ammonium
USABC	United States Advanced Battery Consortium
UV/VIS	ultraviolet-visible
WLF	Williams-Landel-Ferry
XAS	X-ray absorption spectroscopy
XPS	X-ray photoelectron spectroscopy
XRD	X-ray diffraction

ANNUAL REPORTS

1. Exploratory Technology Research Program for Electrochemical Energy Storage – Annual Report for 1997, LBNL-41950 (June 1998).
2. Exploratory Technology Research Program for Electrochemical Energy Storage – Annual Report for 1996, LBNL-40267 (June 1997).
3. Exploratory Technology Research Program for Electrochemical Energy Storage – Annual Report for 1995, LBNL-338842 (June 1996).
4. Exploratory Technology Research Program for Electrochemical Energy Storage – Annual Report for 1994, LBL-37665 (September 1995).
5. Exploratory Technology Research Program for Electrochemical Energy Storage – Annual Report for 1993, LBL-35567 (September 1994).
6. Exploratory Technology Research Program for Electrochemical Energy Storage – Annual Report for 1992, LBL-34081 (October 1993).
7. Exploratory Technology Research Program for Electrochemical Energy Storage – Annual Report for 1991, LBL-32212 (June 1992).
8. Technology Base Research Project for Electrochemical Energy Storage – Annual Report for 1990, LBL-30846 (June 1991).
9. Technology Base Research Project for Electrochemical Energy Storage – Annual Report for 1989, LBL-29155 (May 1990).
10. Technology Base Research Project for Electrochemical Energy Storage – Annual Report for 1988, LBL-27037 (May 1989).
11. Technology Base Research Project for Electrochemical Energy Storage – Annual Report for 1987, LBL-25507 (July 1988).
12. Technology Base Research Project for Electrochemical Energy Storage – Annual Report for 1986, LBL-23495 (July 1987).
13. Technology Base Research Project for Electrochemical Energy Storage – Annual Report for 1985, LBL-21342 (July 1986).
14. Technology Base Research Project for Electrochemical Energy Storage – Annual Report for 1984, LBL-19545 (May 1985).
15. Annual Report for 1983 – Technology Base Research Project for Electrochemical Energy Storage, LBL-17742 (May 1984).
16. Technology Base Research Project for Electrochemical Energy Storage – Annual Report for 1982, LBL-15992 (May 1983).
17. Technology Base Research Project for Electrochemical Energy Storage – Report for 1981, LBL-14305 (June 1982).
18. Applied Battery and Electrochemical Research Program Report for 1981, LBL-14304 (June 1982).
19. Applied Battery and Electrochemical Research Program Report for Fiscal Year 1980, LBL-12514 (April 1981).

SUBCONTRACTOR FINANCIAL DATA - CY 1998

Subcontractor	Principal Investigator	Project	Contract Value (K$)	Term (months)	Expiration Date	Status in CY 1998*
Electrode Characterization						
Lawrence Berkeley National Laboratory	E. Cairns, L. DeJonghe, J. Evans, J. Kerr, K. Kinoshita, F. McLarnon, J. Newman, P. Ross	Electrochemical Energy Storage	1715	12	9-98	C
Lawrence Livermore National Lab.	T. Tran	Li-Ion Carbon Electrode	80	12	12-98	T
University of Michigan	G. Nazri	Carbonaceous Anodes	140	12	9-98	C
Brookhaven National Laboratory	J. McBreen	Battery Materials	136	12	9-98	C
Electrodes for Electrochemical Cells						
Brookhaven National Laboratory	J. Reilly	Metal Hydride Electrodes	200	12	9-98	T
University of South Carolina	R. White	Metal Hydride Properties	90	12	1-99	T
University of Michigan	A.M. Sastry	Novel Cell Components	134	12	9-98	C
Components for Ambient-Temperature Nonaqueous Cells						
SUNY at Binghamton	S. Whittingham	Cathode Materials	65	12	5-99	C
North Carolina State University	S. Khan	Polymer Electrolytes	100	12	9-98	C
Northwestern University	M. Ratner	Polymer Electrolytes	99	12	12-98	C
Delaware State University	K. Wheeler	Transition-Metal Oxides	90	12	7-99	C

* C = continuing, T = terminating


BERKELEY LAB